universität wien

Novel targets and treatments for brain hemorrhage

Ass. Prof. Marietta Zille, PhD

University of Vienna, Department of Pharmaceutical Sciences, Division Pharmacology and Toxicology

Barcelona, October 8, 2024

@ZilleMarietta

Therapeutic targets and approaches in ICH

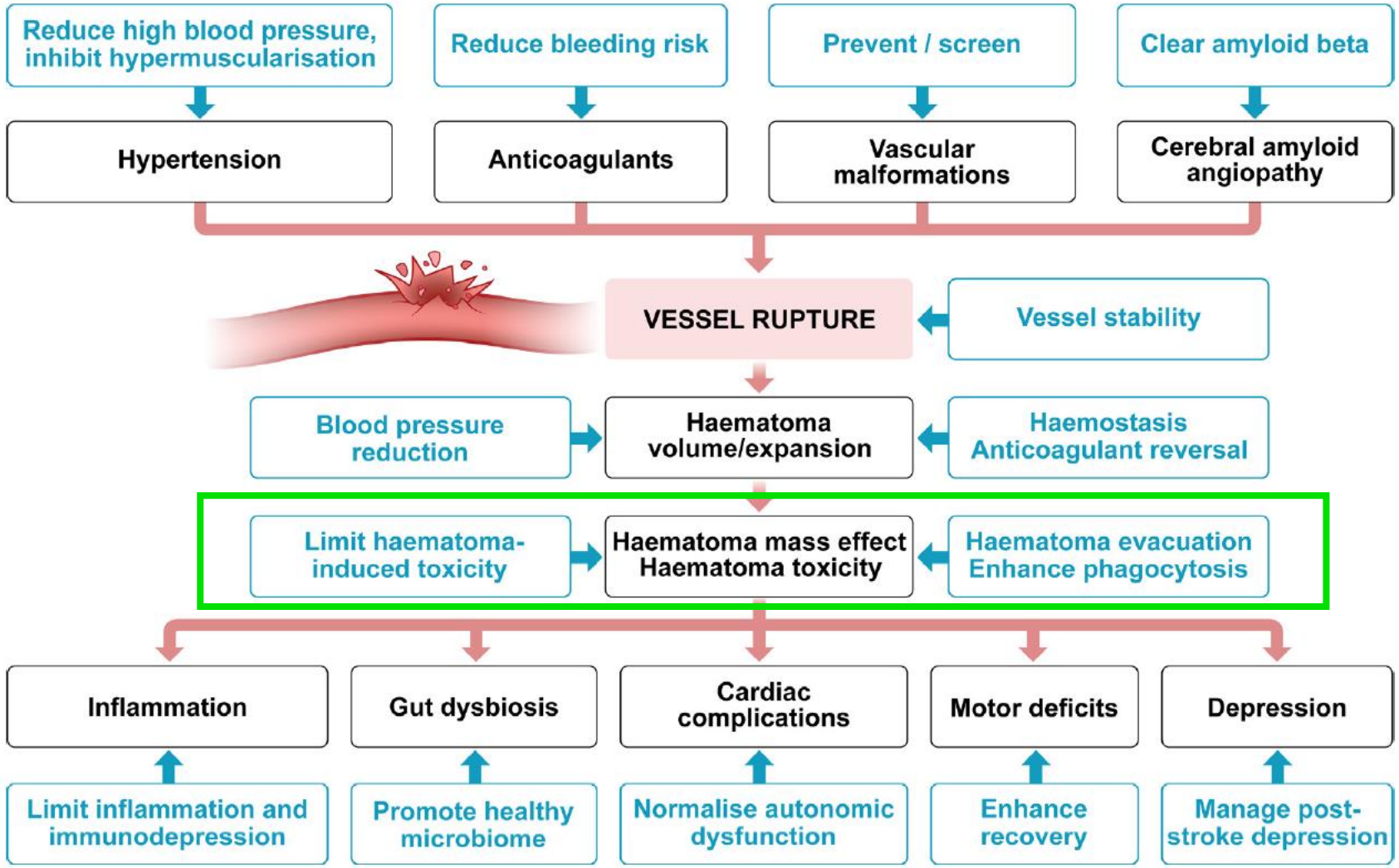

Zille et al., eBioMedicine, 2022

The hematoma as a therapeutic target in ICH

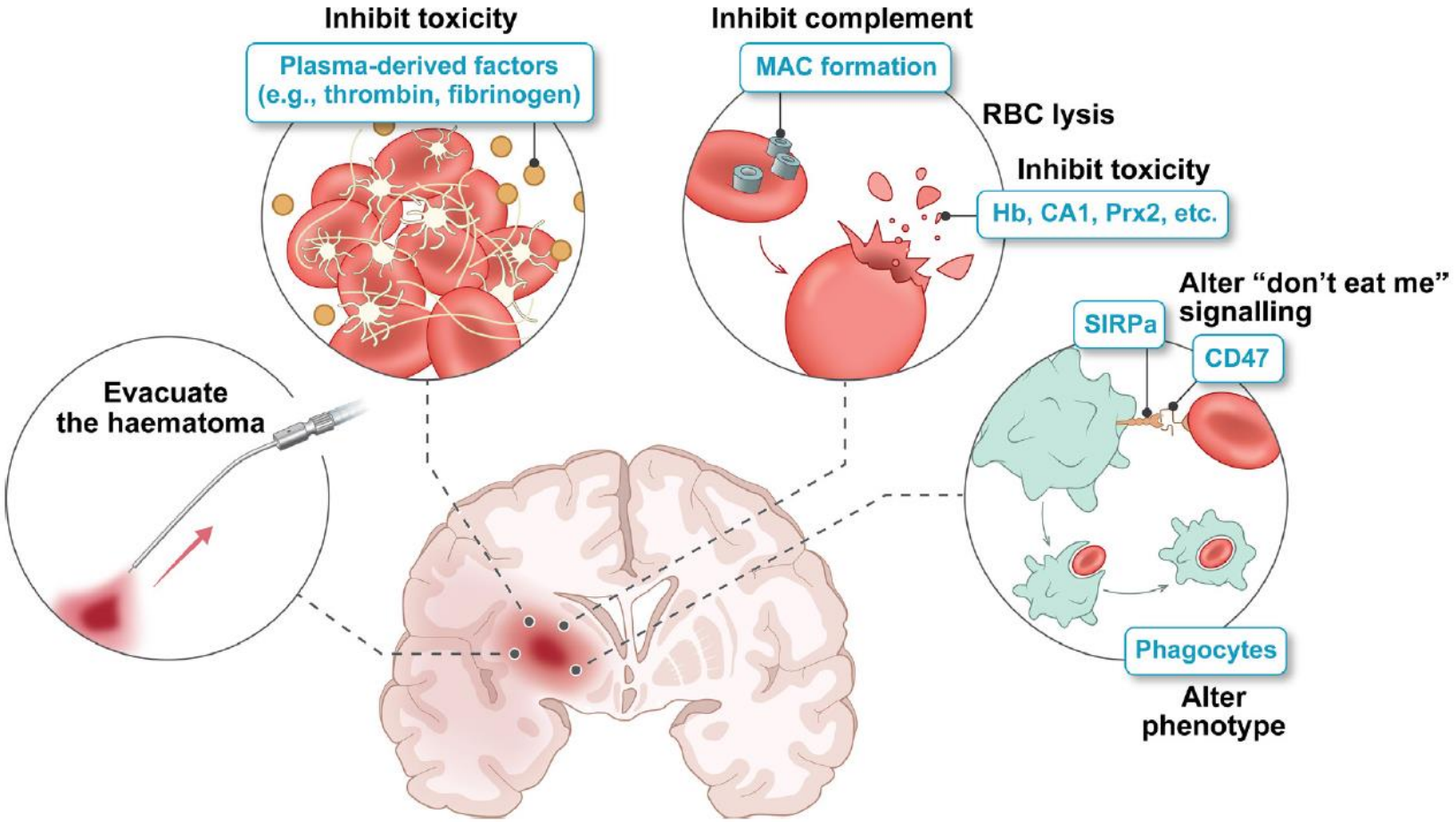

- Retinoid X receptor agonist Bexarotene alters microglia/macrophage phenotype, enhances phagocytosis, speeds hematoma clearance
- Intranasal delivery of IL-4 facilitates microglia- and macrophage-mediated hematoma resolution
- Block 'don't-eat-me' signals expressed on erythrocytes that normally suppress phagocytosis (e.g., using a CD47 antibody)

Zille et al., eBioMedicine, 2022

Hemolysis products mediate secondary injury in ICH

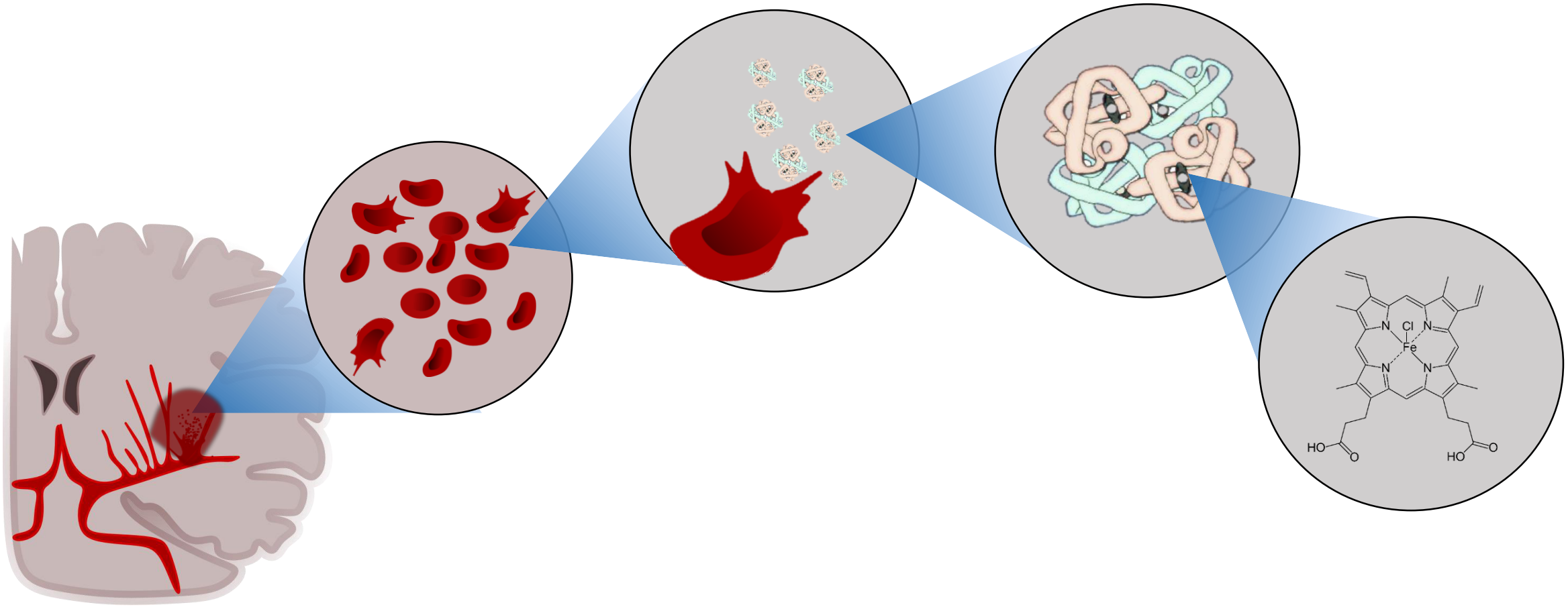

Rupture of blood vessel → Lysis of red blood cells → Hemoglobin breakdown → Heme toxicity → Cell Death

Chen-Roetling and Regan, 2006; Robinson et al., 2009; Wang et al., 2006, Zille et al., 2017

How does lysed blood induce cell death after ICH?

Regulated cell death mechanisms

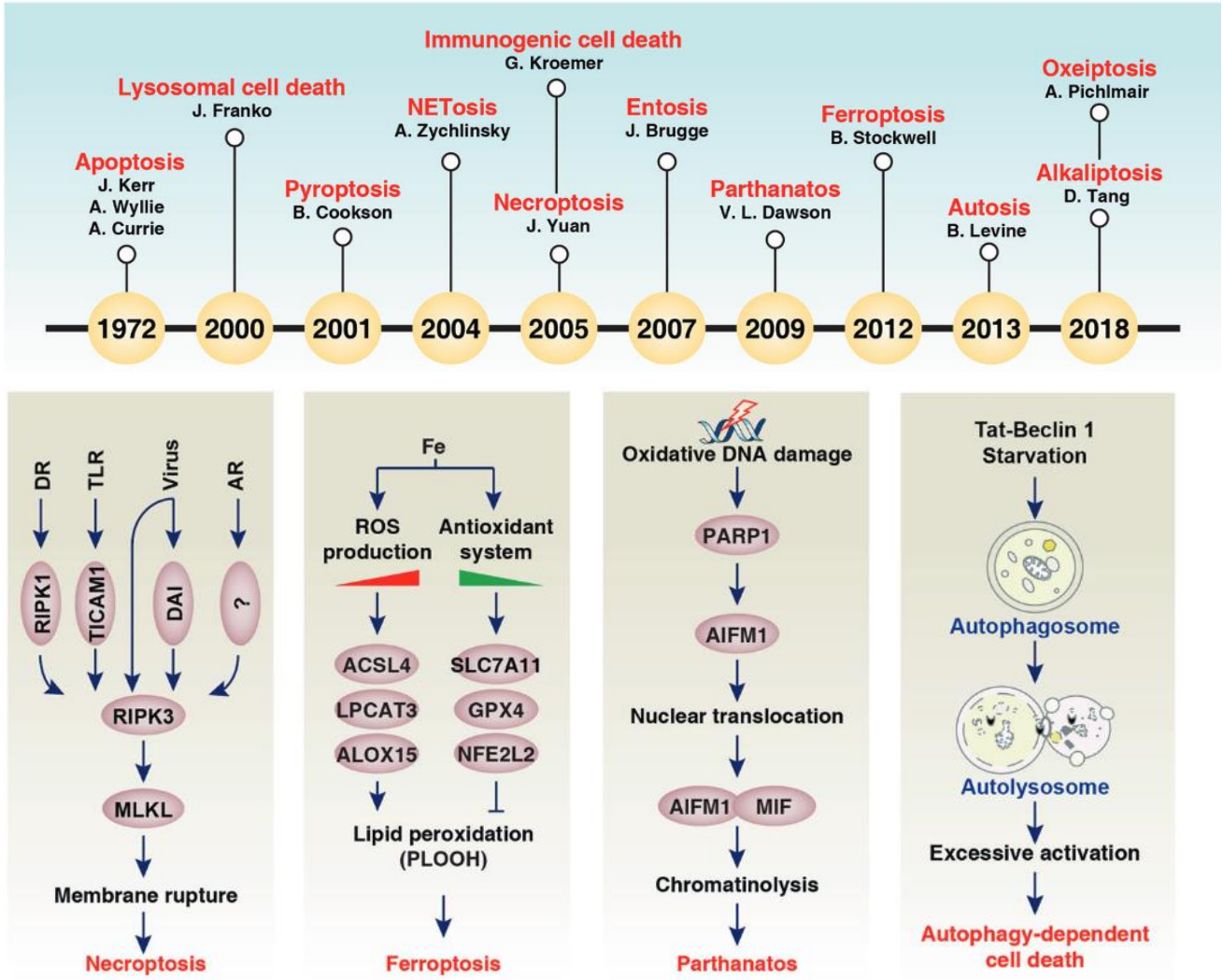

Tang et al., Cell Res, 2019

Model of Hemorrhagic Stroke				
Hemin Toxicity		vehicle		
		100μM hemin		
Cell Death Mechanism	**Subcategory**	**Cell Death Inhibitor**	**Target**	**Conc.**
Autophagy	Macroautophagy	3-Methyladenine	Phosphoinositide 3-kinase (PI3K), autophagosome formation	100-1500μM
		Bafilomycin A1	Endosomal acidification	0.0005-0.1μM
		Chloroquine diphosphate salt	Lysosomal function	0.1-50μM
		Rapamycin	Mechanistic target of rapamycin (mTOR), autophagy inducer	0.1-5μM
	Mitophagy	Mitochondrial division inhibitor 1	GTPase activity in dynamin-related protein Drp-1, abnormal mitophagy	0.1-100μM
Caspase-dependent apoptosis		z-VAD-fmk	Caspases	0.1-100μM
		Cycloheximide	Protein synthesis	0.1-100μM
		Cyclosporine A	Cyclophilin D (mitoch. permeability transition pore)	0.1-10μM
		SB203580	p38 mitogen-activated protein (MAP) kinase (p38)	1-30μM
		SP600125	c-JUN N-terminal kinase (JNK)	0.01-5μM
Regulated Necrosis	Ferroptosis	Cycloheximide	Protein synthesis	0.1-100μM
		Actinomycin D	mRNA synthesis	0.001-1μM
		Ferrostatin-1	Canonical ferroptosis inhibitor, reactive lipid species (RLS)	0.01-1μM
		Deferoxamine	Iron, hypoxia-inducible factor (HIF) prolyl hydroxylase domain-containing (PHD) inhibition	0.1-100μM
		N-Acetylcysteine	Reactive oxygen species (ROS), RLS	100-2000μM
		Trolox, vitamin E analog	RLS	0.1-100μM
		U0126	Mitogen-activated protein kinase kinase 1/2 (MEK 1/2)	1-20μM
	Parthanatos	PARP inhibitor III	Poly(ADP-ribose) polymerase 1 and 2 (PARP1 and 2)	0.1-50μM
		Olaparib (AZD-2281, trade name Lynparza)	PARP1 and 2	1-20μM
	Necroptosis	Necrostatin-1	Receptor-interacting protein kinase 1 (RIP1)	10-250μM

Zille et al., Stroke, 2017

The mechanisms underlying neuronal cell death in hemorrhagic and ischemic stroke are different

Model of Hemorrhagic Stroke					%Viability
Hemin Toxicity		vehicle			100.00
		100μM hemin			50.14 ± 11.89
Cell Death Mechanism	**Subcategory**	**Cell Death Inhibitor**	**Target**	**Conc.**	**%Viability**
Autophagy	Macroautophagy	3-Methyladenine	Phosphoinositide 3-kinase (PI3K), autophagosome formation	100-1500μM	46.62 ± 11.89 (500μM)
		Bafilomycin A1	Endosomal acidification	0.0005-0.1μM	57.42 ± 16.15 (10nM)
		Chloroquine diphosphate salt	Lysosomal function	0.1-50μM	62.87 ± 9.06 (5μM)
		Rapamycin	Mechanistic target of rapamycin (mTOR), autophagy inducer	0.1-5μM	44.34 ± 10.71 (1μM)
	Mitophagy	Mitochondrial division inhibitor 1	GTPase activity in dynamin-related protein Drp-1, abnormal mitophagy	0.1-100μM	53.32 ± 5.59
Caspase-dependent apoptosis		z-VAD-fmk	Caspases	0.1-100μM	45.38 ± 9.87 (100μM)
		Cycloheximide	Protein synthesis	0.1-100μM	47.37 ± 2.78 (100μM)
		Cyclosporine A	Cyclophilin D (mitoch. permeability transition pore)	0.1-10μM	44.2 ± 10.25 (500nM)
		SB203580	p38 mitogen-activated protein (MAP) kinase (p38)	1-30μM	52.61 ± 7.15 (5μM)
		SP600125	c-JUN N-terminal kinase (JNK)	0.01-5μM	65.21 ± 5.78 (30μM)
Regulated Necrosis	Ferroptosis	Cycloheximide	Protein synthesis	0.1-100μM	(0.1μM)
		Actinomycin D	mRNA synthesis	0.001-1μM	53.44 ± 10.79 (1μM)
		Ferrostatin-1	Canonical ferroptosis inhibitor, reactive lipid species (RLS)	0.01-1μM	82.68 ± 11.66 * (1μM)
		Deferoxamine	Iron, hypoxia-inducible factor (HIF) prolyl hydroxylase domain-containing (PHD) inhibition	0.1-100μM	87.14 ± 8.53 * (100μM)
		N-Acetylcysteine	Reactive oxygen species (ROS), RLS	100-2000μM	95.37 ± 7.08 * (1mM)
		Trolox, vitamin E analog	RLS	0.1-100μM	88.3 ± 16.01 * (100μM)
		U0126	Mitogen-activated protein kinase kinase 1/2 (MEK 1/2)	1-20μM	82.45 ± 13.45 * # (10μM)
	Parthanatos	PARP inhibitor III	Poly(ADP-ribose) polymerase 1 and 2 (PARP1 and 2)	0.1-50μM	55.80 ± 12.93 (50μM)
		Olaparib (AZD-2281, trade name Lynparza)	PARP1 and 2	1-20μM	44.64 ± 12.33 (20μM)
	Necroptosis	Necrostatin-1	Receptor-interacting protein kinase 1 (RIP1)	10-250μM	77.4 ± 11.88 * (100μM)

100%

50%

Zille et al., Stroke, 2017

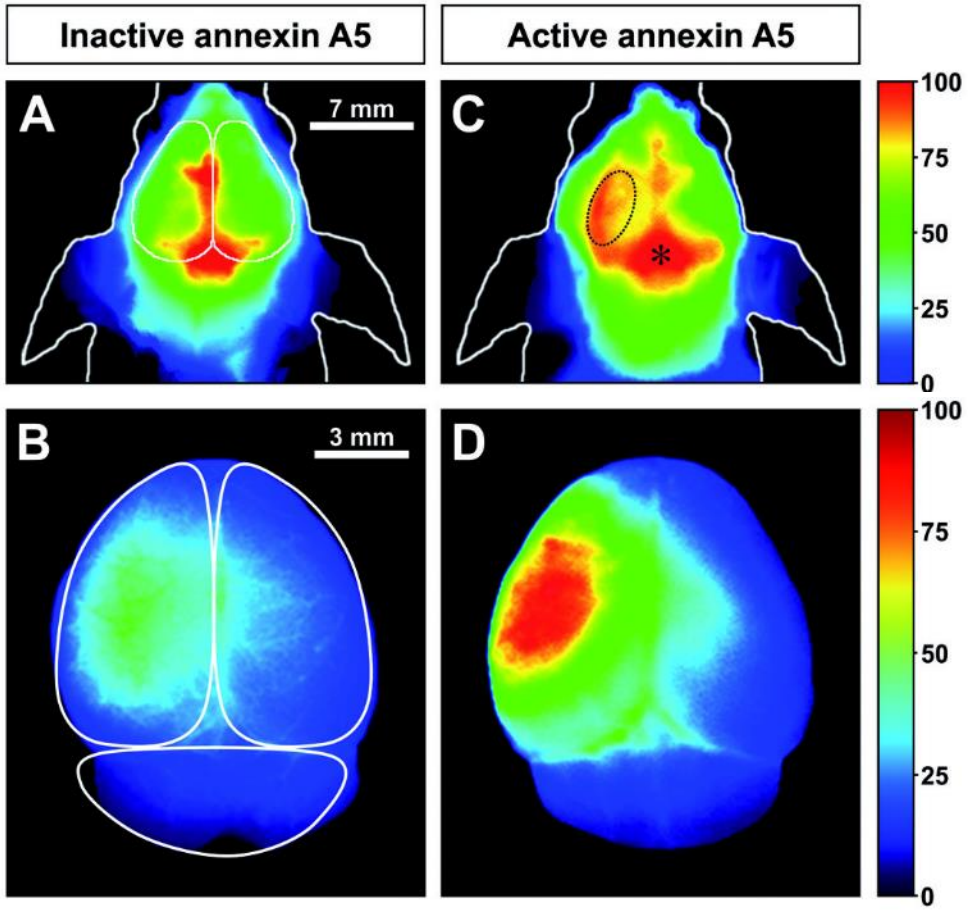

Bahmani, Zille et al., JCBFM, 2011
Riegelsberger, Zille et al., Exp Neurology, 2011;
Zille et al., JCBFM, 2012; Zille et al., Plos One, 2014

Systematic analysis identifies a mixture of cell death pathways in neurons: Necroptosis and ferroptosis

Model of Hemorrhagic Stroke					%Viability
Hemin Toxicity		vehicle			100.00
		100μM hemin			50.14 ± 11.89
Cell Death Mechanism	**Subcategory**	**Cell Death Inhibitor**	**Target**	**Conc.**	**%Viability**
Autophagy	Macroautophagy	3-Methyladenine	Phosphoinositide 3-kinase (PI3K), autophagosome formation	100-1500μM	46.62 ± 11.89 (500μM)
		Bafilomycin A1	Endosomal acidification	0.0005-0.1μM	57.42 ± 16.15 (10nM)
		Chloroquine diphosphate salt	Lysosomal function	0.1-50μM	62.87 ± 9.06 (5μM)
		Rapamycin	Mechanistic target of rapamycin (mTOR), autophagy inducer	0.1-5μM	44.34 ± 10.71 (1μM)
	Mitophagy	Mitochondrial division inhibitor 1	GTPase activity in dynamin-related protein Drp-1, abnormal mitophagy	0.1-100μM	53.32 ± 5.59 (50μM)
Caspase-dependent apoptosis		z-VAD-fmk	Caspases	0.1-100μM	45.38 ± 9.87 (100μM)
		Cycloheximide	Protein synthesis	0.1-100μM	47.37 ± 2.78 (100μM)
		Cyclosporine A	Cyclophilin D (mitoch. permeability transition pore)	0.1-10μM	44.2 ± 10.25 (500nM)
		SB203580	p38 mitogen-activated protein (MAP) kinase (p38)	1-30μM	52.61 ± 7.15 (5μM)
		SP600125	c-JUN N-terminal kinase (JNK)	0.01-5μM	65.21 ± 5.78 (30μM)
		Cycloheximide	Protein synthesis	0.1-100μM	47.37 ± 2.78 (0.1μM)
		Actinomycin D	mRNA synthesis	0.001-1μM	53.44 ± 10.79 (1μM)
Regulated Necrosis	Ferroptosis	Ferrostatin-1	Canonical ferroptosis inhibitor, reactive lipid species (RLS)	0.01-1μM	82.68 ± 11.66 * (1μM)
		Deferoxamine	Iron, hypoxia-inducible factor (HIF) prolyl hydroxylase domain-containing (PHD) inhibition	0.1-100μM	87.14 ± 8.53 * (100μM)
		N-Acetylcysteine	Reactive oxygen species (ROS), RLS	100-2000μM	95.37 ± 7.08 * (1mM)
		Trolox, vitamin E analog	RLS	0.1-100μM	88.3 ± 16.01 * (100μM)
		U0126	Mitogen-activated protein kinase kinase 1/2 (MEK 1/2)	1-20μM	82.45 ± 13.45 * # (10μM)
	Parthanatos	PARP inhibitor III	Poly(ADP-ribose) polymerase 1 and 2 (PARP1 and 2)	0.1-50μM	55.80 ± 12.93 (50μM)
		Olaparib (AZD-2281, trade name Lynparza)	PARP1 and 2	1-20μM	44.64 ± 12.33 (20μM)
	Necroptosis	Necrostatin-1	Receptor-interacting protein kinase 1 (RIP1)	10-250μM	77.4 ± 11.88 * (100μM)

100%

50%

Ultrastructural Characteristics of Neuronal Death and White Matter Injury in Mouse Brain Tissues After Intracerebral Hemorrhage: Coexistence of Ferroptosis, Autophagy, and Necrosis

Qian Li[1,2,3†], Abigail Weiland[1†], Xuemei Chen[4], Xi Lan[1], Xiaoning Han[1], Frederick Durham[1], Xi Liu[1], Jieru Wan[1], Wendy C. Ziai[1,5], Daniel F. Hanley[5] and Jian Wang[1]*

Front Neurol, 2018

Stroke

ORIGINAL CONTRIBUTION

Neuronal Death After Hemorrhagic Stroke In Vitro and In Vivo Shares Features of Ferroptosis and Necroptosis

Marietta Zille, Saravanan S. Karuppagounder, Yingxin Chen, Peter J. Gough, John Bertin, Joshua Finger, Teresa A. Milner, Elizabeth A. Jonas, Rajiv R. Ratan

2017

Ferroptosis

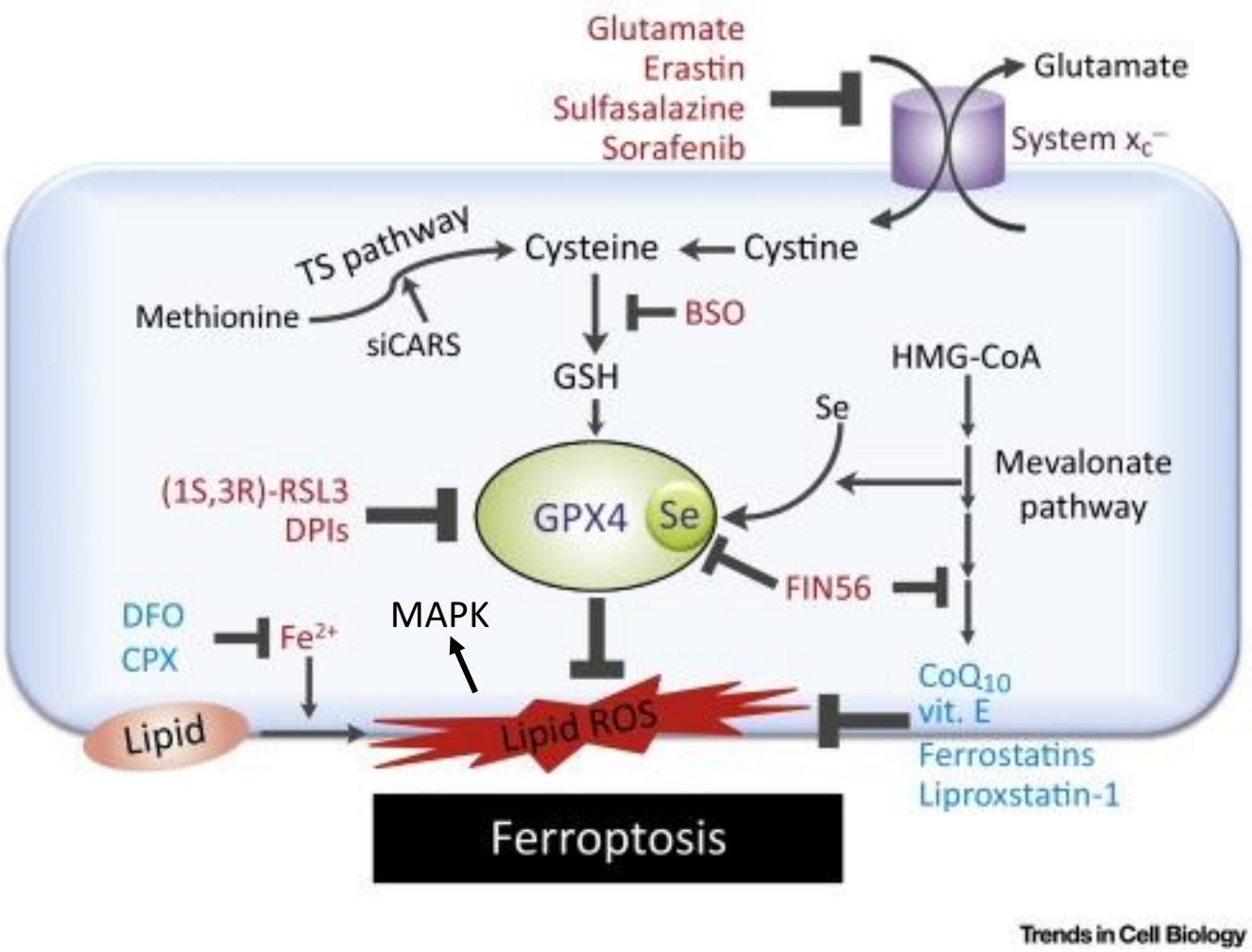

- Iron-dependent form of non-apoptotic cell death
- Accumulation of lipid peroxidation products
- Involvement of glutathione peroxidase 4 (GPX4)
- Activation of Mitogen-activated protein kinase (MAPK)
- Lack of blebbing of the plasma membrane

Adapted from Yang and Stockwell, Trends in Cell Biology, 2016

Evidence of ferroptosis in ICH: Induction of 5-lipoxygenase (ALOX5)-dependent oxidized lipids

- Iron-dependent form of non-apoptotic cell death
- **Accumulation of lipid peroxidation products**
- Involvement of glutathione peroxidase 4 (GPX4)
- Activation of Mitogen-activated protein kinase (MAPK)
- Lack of blebbing of the plasma membrane

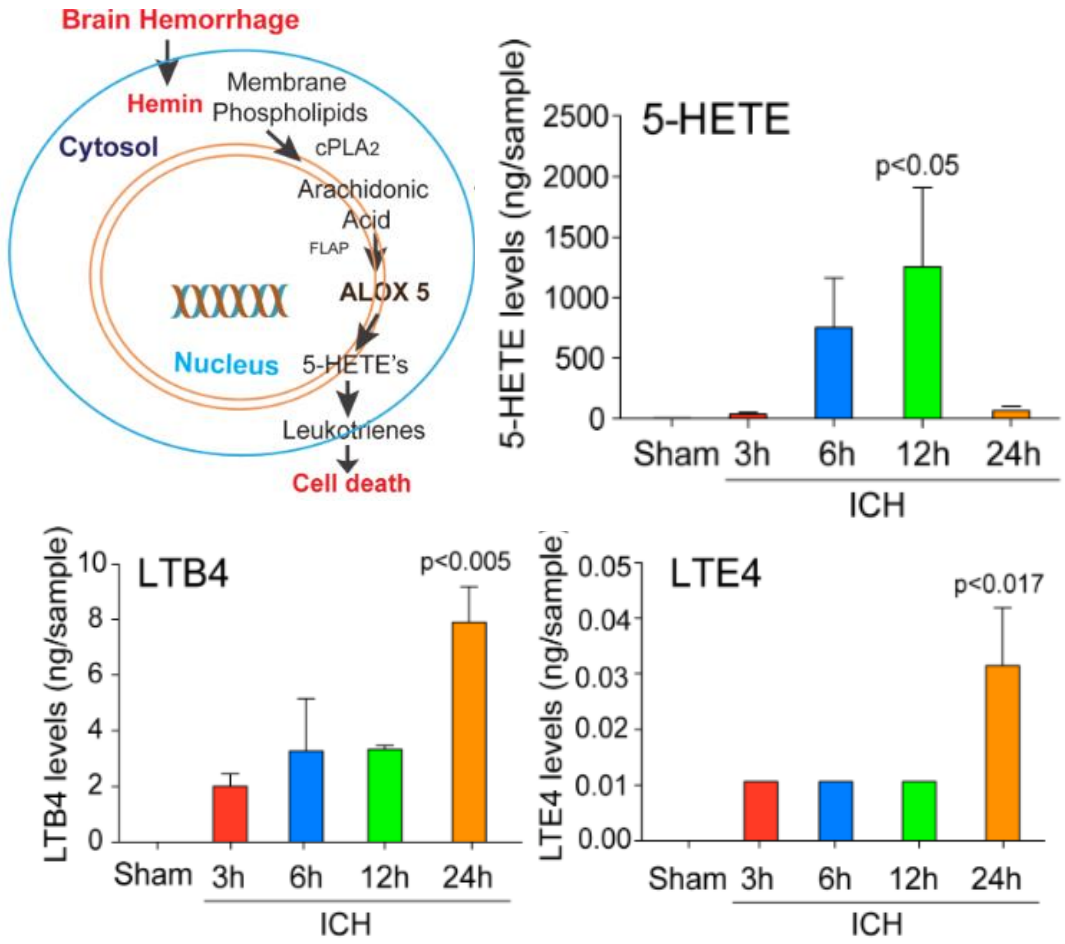

Karuppagounder et al., Ann Neurol, 2018

5-HETE – 5-hydroxyeicosatetraenoic acid, LTB4 – Leukotriene B4, LTE4 – Leukotriene E4

Evidence of ferroptosis in ICH: Stabilizing GPX4 rescues neurons from hemin-induced toxicity

- Iron-dependent form of non-apoptotic cell death
- Accumulation of lipid peroxidation products
- **Involvement of glutathione peroxidase 4 (GPX4)**
- Activation of Mitogen-activated protein kinase (MAPK)
- Lack of blebbing of the plasma membrane

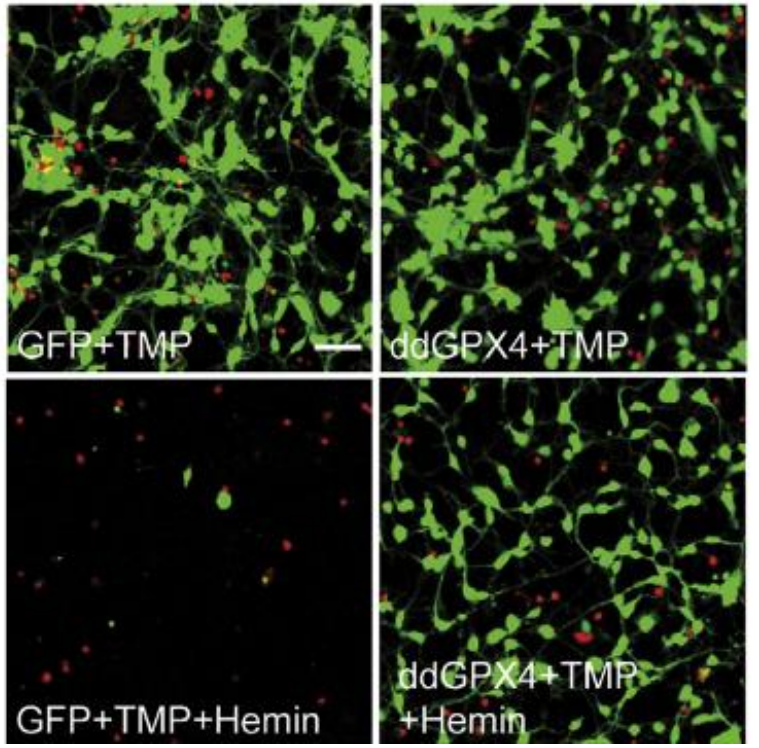

Alim et al., Cell, 2019

Evidence of ferroptosis in ICH: Inducing GPX4 leads to improved outcome *in vivo*

- Iron-dependent form of non-apoptotic cell death
- Accumulation of lipid peroxidation products
- **Involvement of glutathione peroxidase 4 (GPX4)**
- Activation of Mitogen-activated protein kinase (MAPK)
- Lack of blebbing of the plasma membrane

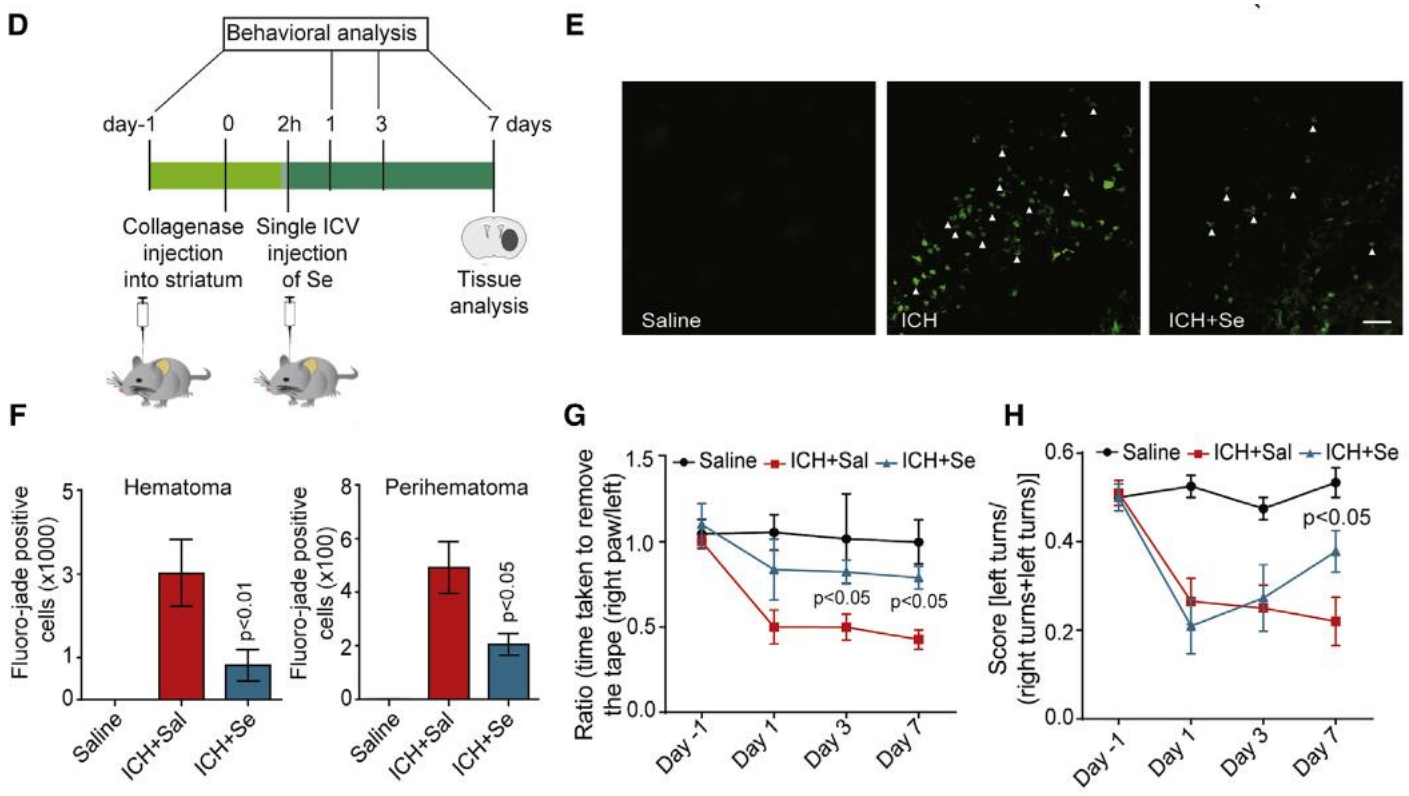

Alim et al., Cell, 2019

Evidence of ferroptosis in ICH: Induction of ERK1/2 phosphorylation

- Iron-dependent form of non-apoptotic cell death
- Accumulation of lipid peroxidation products
- Involvement of glutathione peroxidase 4 (GPX4)
- **Activation of Mitogen-activated protein kinase (MAPK)**
- Lack of blebbing of the plasma membrane

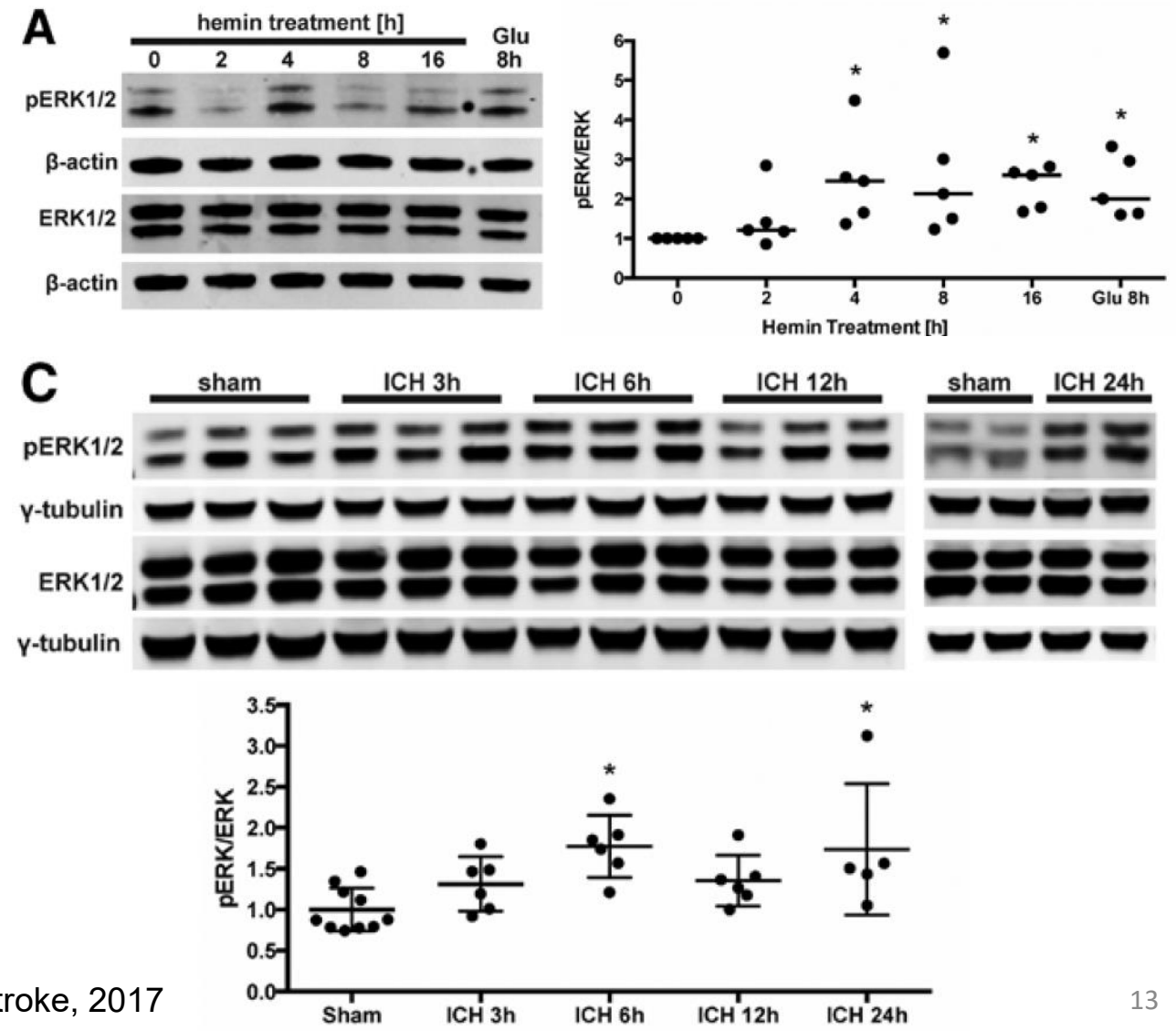

Zille et al., Stroke, 2017

Evidence of ferroptosis in ICH: Necrotic phenotype

- Iron-dependent form of non-apoptotic cell death
- Accumulation of lipid peroxidation products
- Involvement of glutathione peroxidase 4 (GPX4)
- Activation of Mitogen-activated protein kinase (MAPK)
- **Lack of blebbing of the plasma membrane**

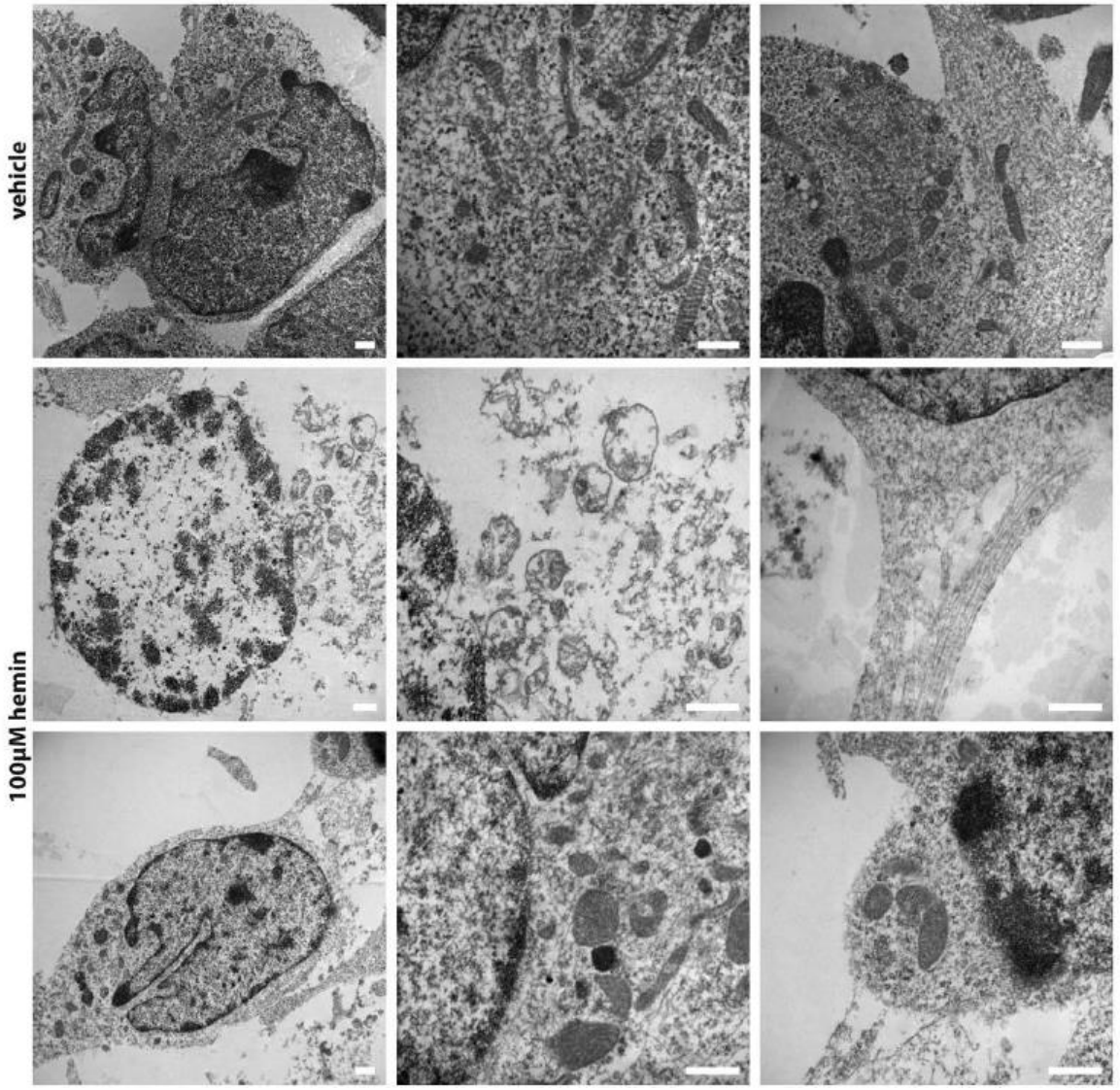

Zille et al., Stroke, 2017

Classical, glutathione depletion-induced ferroptosis vs. hemin-induced ferroptosis

Criterion	Classical, glutathione depletion-induced ferroptosis	Hemin-induced ferroptosis
Reactive lipid species-dependent	+	+
Glutathione enhancing agents are protective	+	+
GPX4 forced expression is protective	+	+
Iron chelators are protective	+	+
ERK1/2 hyperactivation	+	+
12/15-lipoxygenase-dependent	+	-
Transcription-dependent	+	-
Nuclear translocation of phospho-ERK1/2	+	-
Mkp3 forced expression is protective	+	-

Zille et al., J Neurosci, 2022

Unbiased phosphoproteomics identifies different signatures in hemin- vs. erastin-induced ferroptosis

A

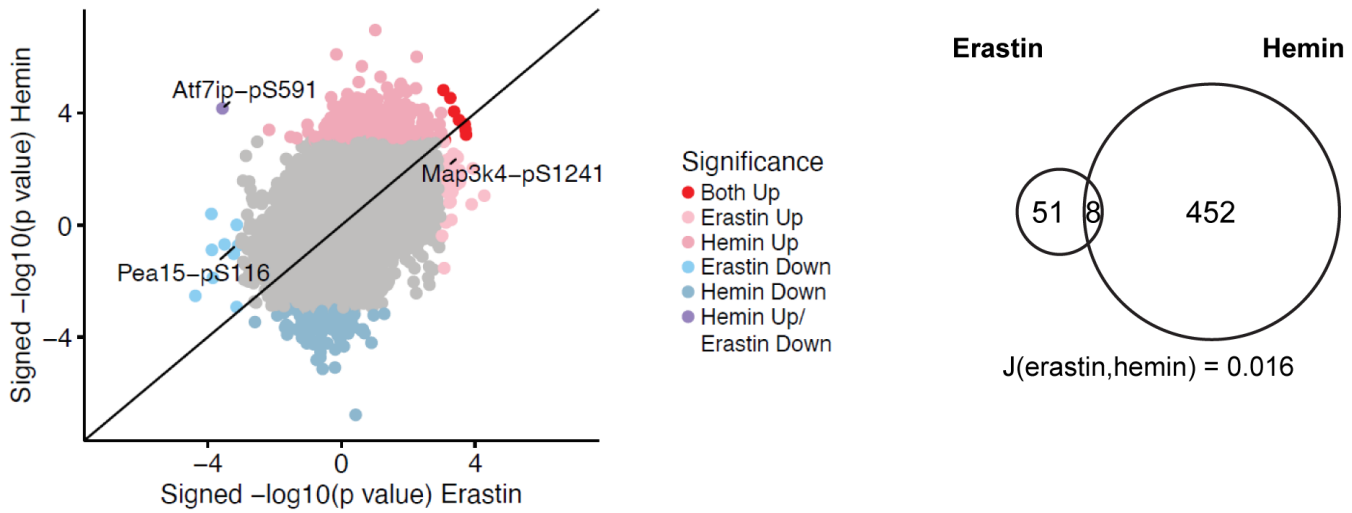

- 28022 phosphopeptides from 4871 proteins
- 452 peptides from 369 proteins altered after 5h hemin treatment
- 51 peptides from 49 proteins altered after 7h erastin treatment
- Only 9 peptides changed in both sets, of which 8 in the same direction

B

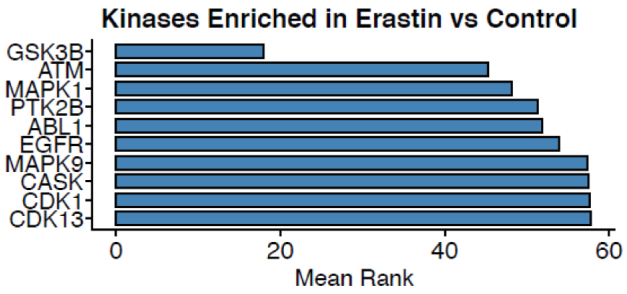

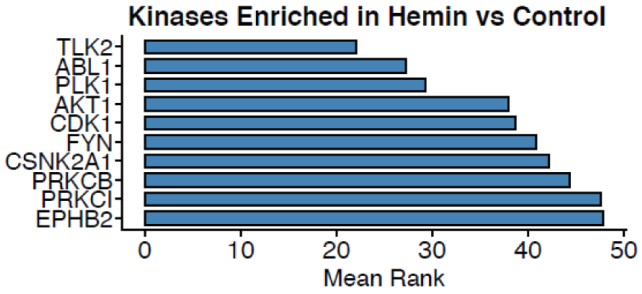

- KEA3 analysis
- Low ranks suggest greater enrichment
- MAPK1 enriched in erastin but not hemin treatment
- TLK2 and AKT1 among top 10 in hemin but not erastin treatment

Zille et al., J Neurosci, 2022

Ferroptosis inhibitors block hemin-induced neuronal death

Model of Hemorrhagic Stroke					%Viability
Hemin Toxicity		vehicle			100.00
		100μM hemin			50.14 ± 11.89
Cell Death Mechanism	**Subcategory**	**Cell Death Inhibitor**	**Target**	**Conc.**	**%Viability**
Autophagy	Macroautophagy	3-Methyladenine	Phosphoinositide 3-kinase (PI3K), autophagosome formation	100-1500μM	46.62 ± 11.89 (500μM)
		Bafilomycin A1	Endosomal acidification	0.0005-0.1μM	57.42 ± 16.15 (10nM)
		Chloroquine diphosphate salt	Lysosomal function	0.1-50μM	62.87 ± 9.06 (5μM)
		Rapamycin	Mechanistic target of rapamycin (mTOR), autophagy inducer	0.1-5μM	44.34 ± 10.71 (1μM)
	Mitophagy	Mitochondrial division inhibitor 1	GTPase activity in dynamin-related protein Drp-1, abnormal mitophagy	0.1-100μM	53.32 ± 5.59 (50μM)
Caspase-dependent apoptosis		z-VAD-fmk	Caspases	0.1-100μM	45.38 ± 9.87 (100μM)
		Cycloheximide	Protein synthesis	0.1-100μM	47.37 ± 2.78 (100μM)
		Cyclosporine A	Cyclophilin D (mitoch. permeability transition pore)	0.1-10μM	44.2 ± 10.25 (500nM)
		SB203580	p38 mitogen-activated protein (MAP) kinase (p38)	1-30μM	52.61 ± 7.15 (5μM)
		SP600125	c-JUN N-terminal kinase (JNK)	0.01-5μM	65.21 ± 5.78 (30μM)
Regulated Necrosis	Ferroptosis	Cycloheximide	Protein synthesis	0.1-100μM	47.37 ± 2.78 (0.1μM)
		Actinomycin D	mRNA synthesis	0.001-1μM	53.44 ± 10.79 (1μM)
		Ferrostatin-1	Canonical ferroptosis inhibitor, reactive lipid species (RLS)	0.01-1μM	82.68 ± 11.66 * (1μM)
		Deferoxamine	Iron, hypoxia-inducible factor (HIF) prolyl hydroxylase domain-containing (PHD) inhibition	0.1-100μM	87.14 ± 8.53 * (100μM)
		N-Acetylcysteine	Reactive oxygen species (ROS), RLS	100-2000μM	95.37 ± 7.08 * (1mM)
		Trolox, vitamin E analog	RLS	0.1-100μM	88.3 ± 16.01 * (100μM)
		U0126	Mitogen-activated protein kinase kinase 1/2 (MEK 1/2)	1-20μM	82.45 ± 13.45 * # (10μM)
	Parthanatos	PARP inhibitor III	Poly(ADP-ribose) polymerase 1 and 2 (PARP1 and 2)	0.1-50μM	55.80 ± 12.93 (50μM)
		Olaparib (AZD-2281, trade name Lynparza)	PARP1 and 2	1-20μM	44.64 ± 12.33 (20μM)
	Necroptosis	Necrostatin-1	Receptor-interacting protein kinase 1 (RIP1)	10-250μM	77.4 ± 11.88 * (100μM)

100%

50%

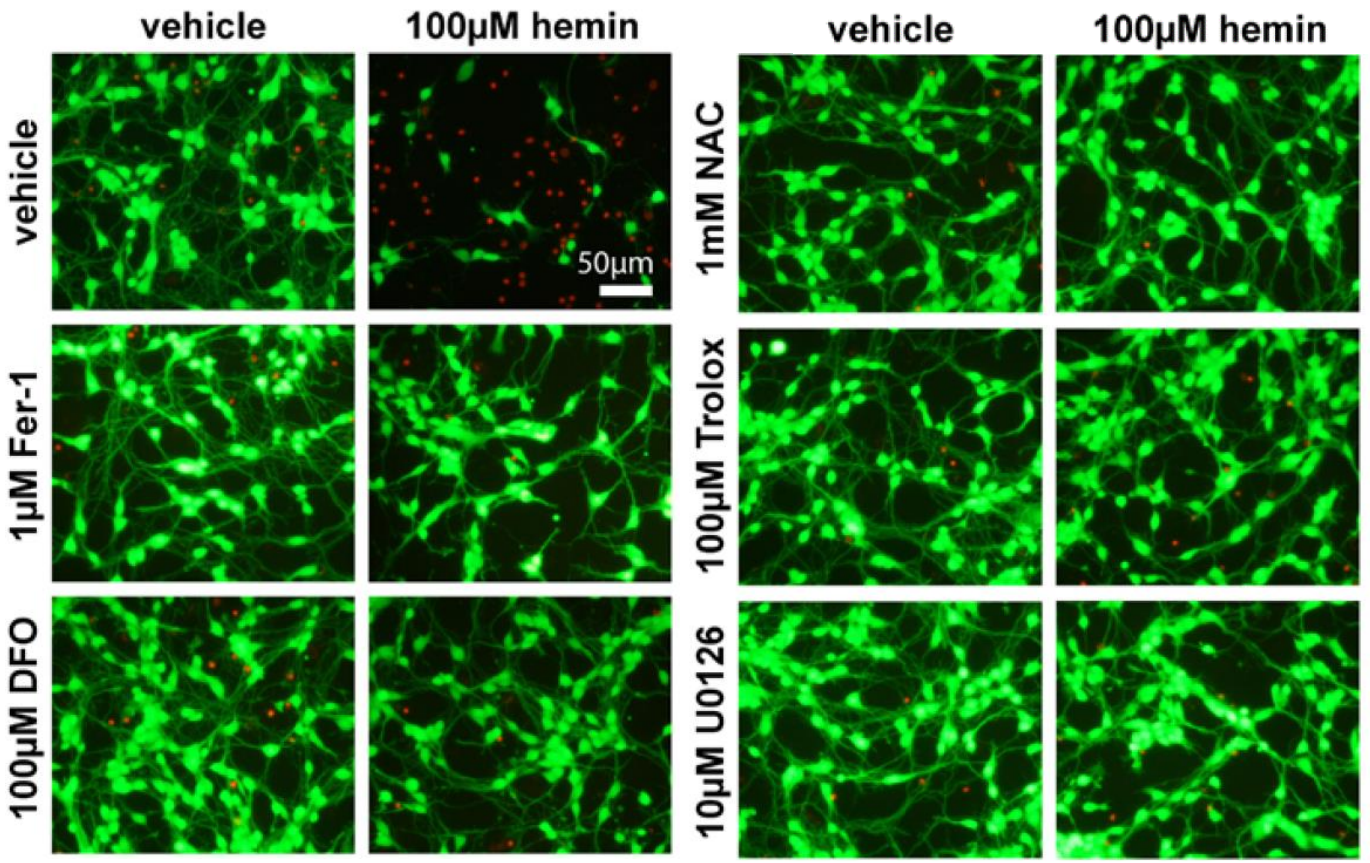

Zille et al., Stroke, 2017

Studying the rich biology of these pathways gives rise to therapeutics

Model of Hemorrhagic Stroke					%Viability
Hemin Toxicity		vehicle			100.00
		100μM hemin			50.14 ± 11.89
Cell Death Mechanism	Subcategory	Cell Death Inhibitor	Target	Conc.	%Viability
Autophagy	Macroautophagy	3-Methyladenine	Phosphoinositide 3-kinase (PI3K), autophagosome formation	100-1500μM	46.62 ± 11.89 (500μM)
		Bafilomycin A1	Endosomal acidification	0.0005-0.1μM	57.42 ± 16.15 (10nM)
		Chloroquine diphosphate salt	Lysosomal function	0.1-50μM	62.87 ± 9.06 (5μM)
		Rapamycin	Mechanistic target of rapamycin (mTOR), autophagy inducer	0.1-5μM	44.34 ± 10.71 (1μM)
	Mitophagy	Mitochondrial division inhibitor 1	GTPase activity in dynamin-related protein Drp-1, abnormal mitophagy	0.1-100μM	53.32 ± 5.59 (50μM)
Caspase-dependent apoptosis		z-VAD-fmk	Caspases	0.1-100μM	45.38 ± 9.87 (100μM)
		Cycloheximide	Protein synthesis	0.1-100μM	47.37 ± 2.78 (100μM)
		Cyclosporine A	Cyclophilin D (mitoch. permeability transition pore)	0.1-10μM	44.2 ± 10.25 (500nM)
		SB203580	p38 mitogen-activated protein (MAP) kinase (p38)	1-30μM	52.61 ± 7.15 (5μM)
		SP600125	c-JUN N-terminal kinase (JNK)	0.01-5μM	65.21 ± 5.78 (30μM)
Regulated Necrosis	Ferroptosis	Cycloheximide	Protein synthesis	0.1-100μM	47.37 ± 2.78 (0.1μM)
		Actinomycin D	mRNA synthesis	0.001-1μM	53.44 ± 10.79 (1μM)
		Ferrostatin-1	Canonical ferroptosis inhibitor, reactive lipid species (RLS)	0.01-1μM	82.68 ± 11.66 * (1μM)
		Deferoxamine	Iron, hypoxia-inducible factor (HIF) prolyl hydroxylase domain-containing (PHD) inhibition	0.1-100μM	87.14 ± 8.53 * (100μM)
		N-Acetylcysteine	Reactive oxygen species (ROS), RLS	100-2000μM	95.37 ± 7.08 * (1mM)
		Trolox, vitamin E analog	RLS	0.1-100μM	88.5 ± 10.81 * (100μM)
		U0126	Mitogen-activated protein kinase kinase 1/2 (MEK 1/2)	1-20μM	82.45 ± 13.45 * # (10μM)
	Parthanatos	PARP inhibitor III	Poly(ADP-ribose) polymerase 1 and 2 (PARP1 and 2)	0.1-50μM	55.80 ± 12.93 (50μM)
		Olaparib (AZD-2281, trade name Lynparza)	PARP1 and 2	1-20μM	44.64 ± 12.33 (20μM)
	Necroptosis	Necrostatin-1	Receptor-interacting protein kinase 1 (RIP1)	10-250μM	77.4 ± 11.88 * (100μM)

100%

50%

Zille et al., Stroke, 2017

Inhibition of neuronal ferroptosis protects hemorrhagic brain

Qian Li, … , Brent R. Stockwell, Jian Wang

JCI Insight. 2017;2(7):e90777. https://doi.org/10.1172/jci.insight.90777.

Deferoxamine mesylate in patients with intracerebral haemorrhage (i-DEF): a multicentre, randomised, placebo-controlled, double-blind phase 2 trial

*Magdy Selim, Lydia D Foster, Claudia S Moy, Guohua Xi, Michael D Hill, Lewis B Morgenstern, Steven M Greenberg, Michael L James, Vineeta Singh, Wayne M Clark, Casey Norton, Yuko Y Palesch, Sharon D Yeatts, on behalf of the i-DEF Investigators**

iDEF
Intracerebral Hemorrhage Deferoxamine Trial

Lancet Neurology, 2019

N-Acetylcysteine Targets 5 Lipoxygenase-Derived, Toxic Lipids and Can Synergize With Prostaglandin E_2 to Inhibit Ferroptosis and Improve Outcomes Following Hemorrhagic Stroke in Mice

Saravanan S. Karuppagounder, PhD,[1,2] Lauren Alin, BS,[1,2] Yingxin Chen, MD,[1,2] David Brand, BS,[1,2] Megan W. Bourassa, PhD,[1,2] Kristen Dietrich, BS[3]

Annals of Neurology, 2018

Hemin-Induced Death Models Hemorrhagic Stroke and Is a Variant of Classical Neuronal Ferroptosis

https://doi.org/10.1523/JNEUROSCI.0923-20.2021

Cite as: J. Neurosci 2022; 10.1523/JNEUROSCI.0923-20.2021

What about other cell types in the brain?

Systematic literature review on brain endothelial cell death in stroke

cell stress

Review

www.cell-stress.com

2019

The impact of endothelial cell death in the brain and its role after stroke: A systematic review

Marietta Zille[1,*], Maulana Ikhsan[1], Yun Jiang[1,2], Josephine Lampe[1,2], Jan Wenzel[1,2] and Markus Schwaninger[1,2,*]

- Brain endothelial cell death occurs both rapidly and at later time points
- Cell death signaling is complex and includes multiple cell death subroutines (apoptosis, autophagy, necroptosis, and maybe ferroptosis)
- Data on brain endothelial cell death after brain hemorrhage is limited

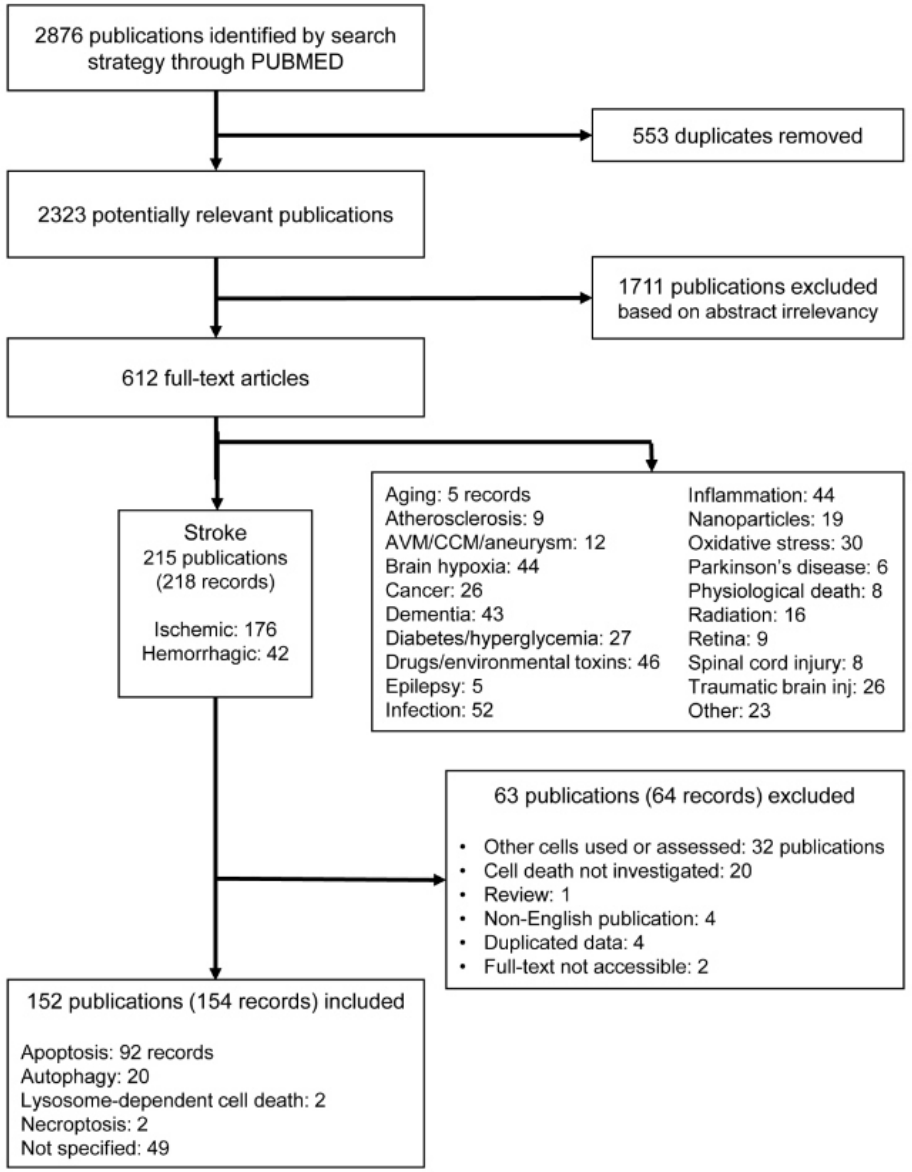

Hemin induces brain endothelial cell death

350µM hemin

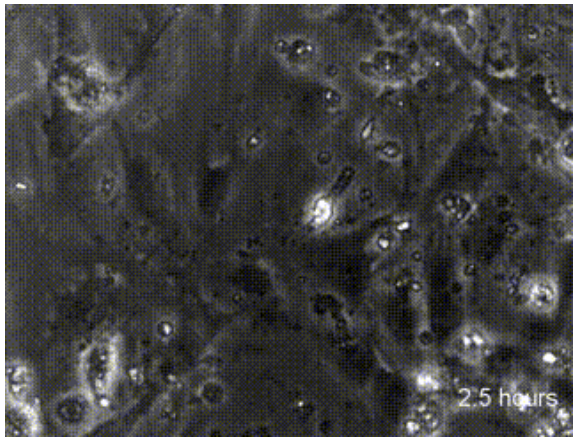

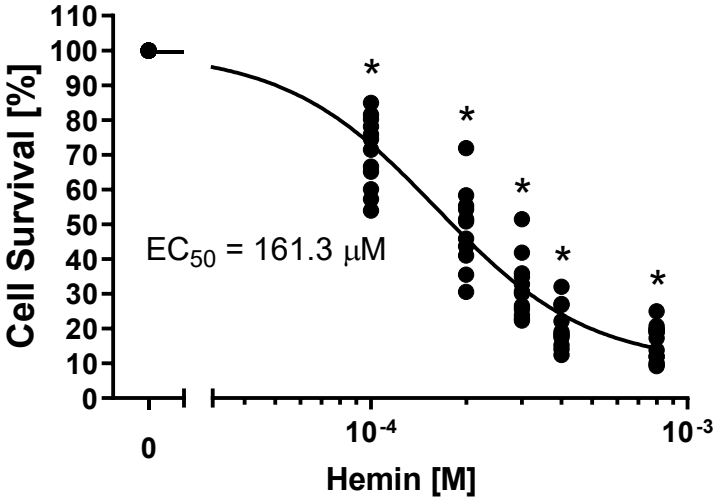

Svenja Landt Maulana Ikhsan

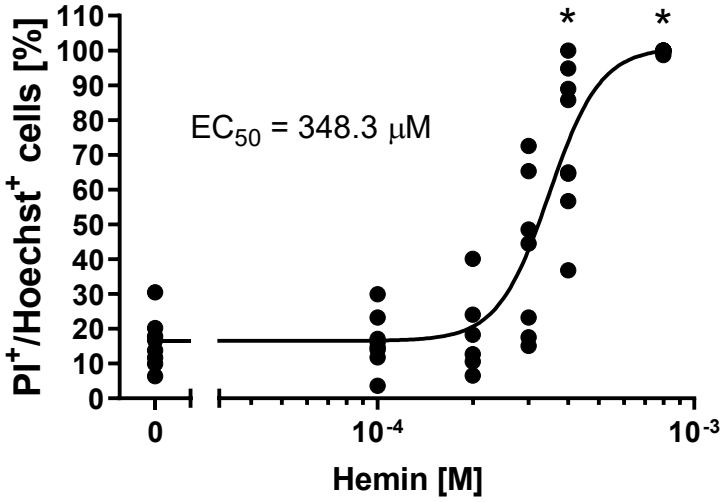

unpublished data

Hemin-induced brain EC death is partially rescued by ferroptosis inhibitors and MDA expression is increased

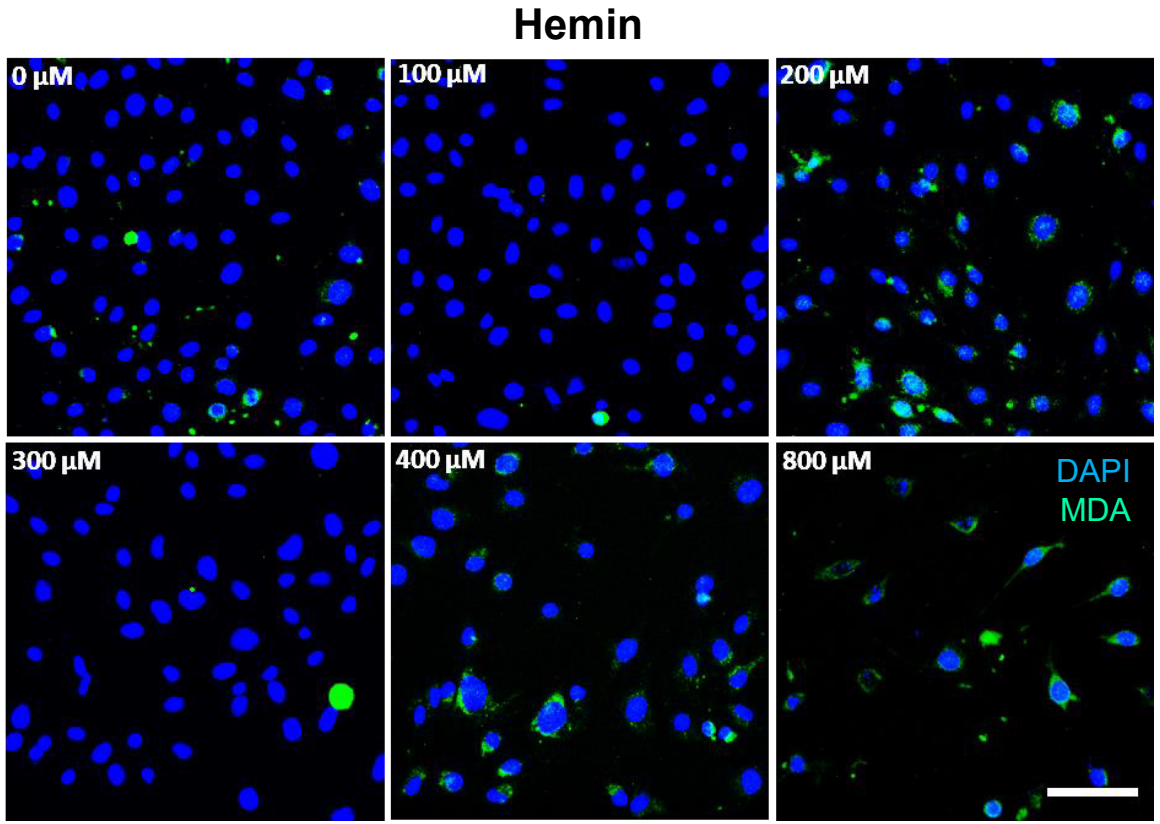

Model of hemorrhagic stroke				Viability [%]
Hemin toxicity	Vehicle			100
	350 µM hemin			18.85 (17.84)
Cell death mechanism	**Cell death inhibitor**	**Target**	**Conc.**	**Viability [%]**
Ferroptosis	Actinomycin D	mRNA synthesis	1 µM	20.50 (20.38)
	Cycloheximide	Protein Synthesis	100 µM	16.36 (7.53)*
	Ferrostatin-1	Canonical ferroptosis inhibitor, reactive lipid species (RLS)	1 µM	20.17 (14.81)
	Deferoxamine	Iron, hypoxia induced factor (HIF) prolyl hydroxylase domain-containing inhibition	100 µM	42.60 (25.08)*
	N-Acetylcysteine	Reactive oxygen species (ROS), RLS	2000 µM	43.83 (17.14)*
	Trolox, vitamin E analog	RLS	100 µM	42.00 (31.09)*
	U0126	Mitogen activated protein kinase kinase 1/2 (MEK 1/2)	20 µM	23.83 (23.03)
	U0124	U0126 inactive control	20 µM	37.734 (13.924)

100%
20%

unpublished data

What is the contribution of axonal degeneration in ICH?

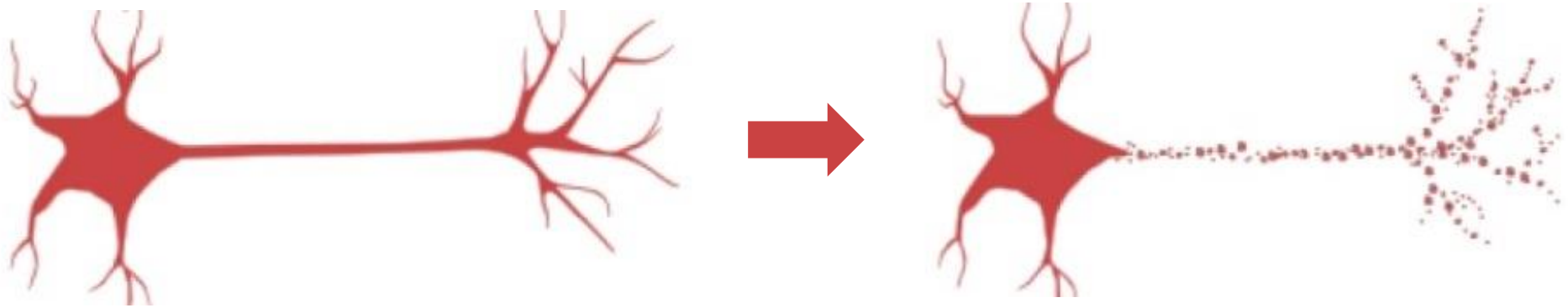

Systematic literature review on axonal degeneration in brain hemorrhage

- Occurs in patients as early as 24 h and in animal models as early as 6 h
- Correlates with hematoma volume and worsening of clinical outcomes
- Occurs in various locations, especially in the hemorrhagic center and perihemorrhagic zone
- Extent increases over time
- Beneficial therapeutic interventions:
  - Target neuroinflammation
  - Improve energy metabolism
  - Inhibit microtubule breakdown
  - Stimulate axonal growth and regeneration

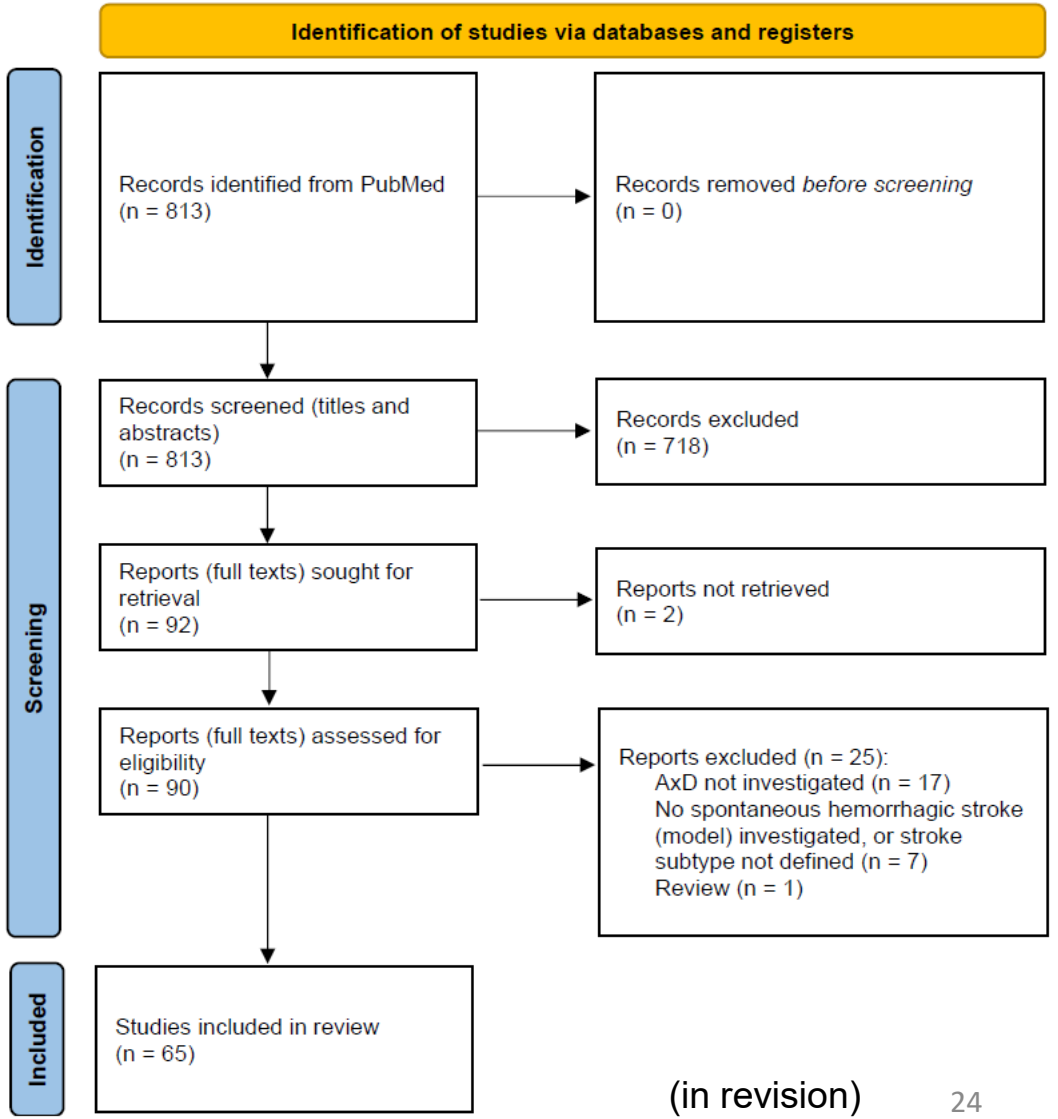

(in revision)

Studying axonal degeneration after brain hemorrhage

Alex Palumbo

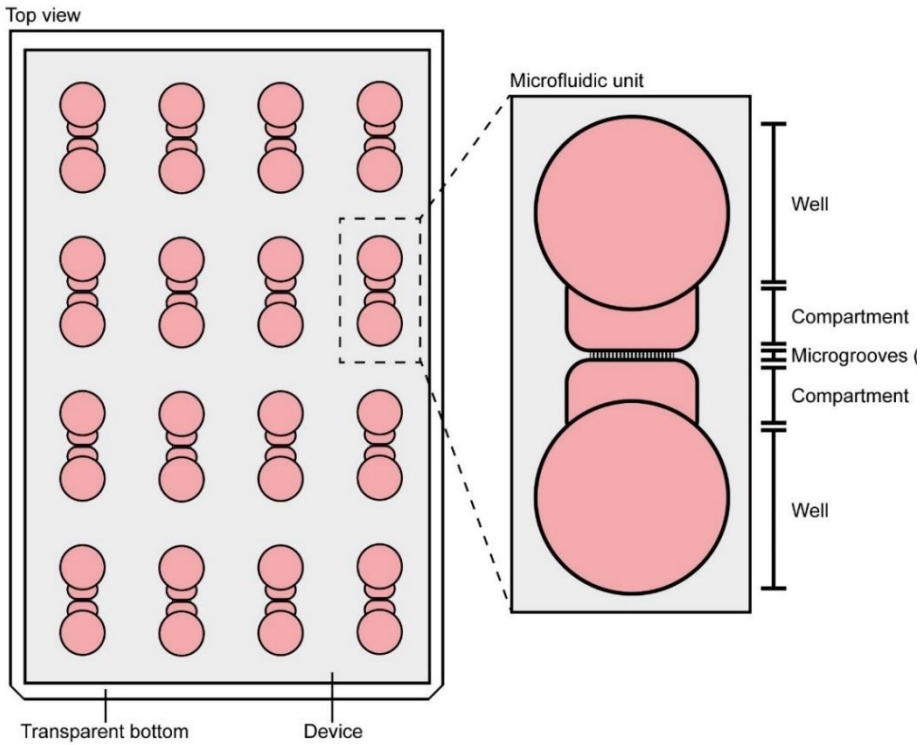

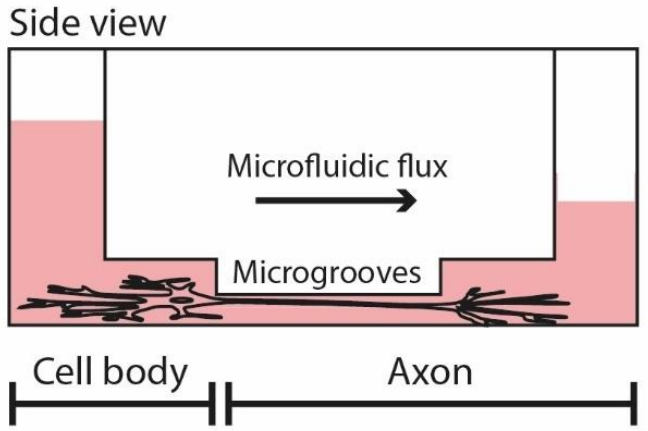

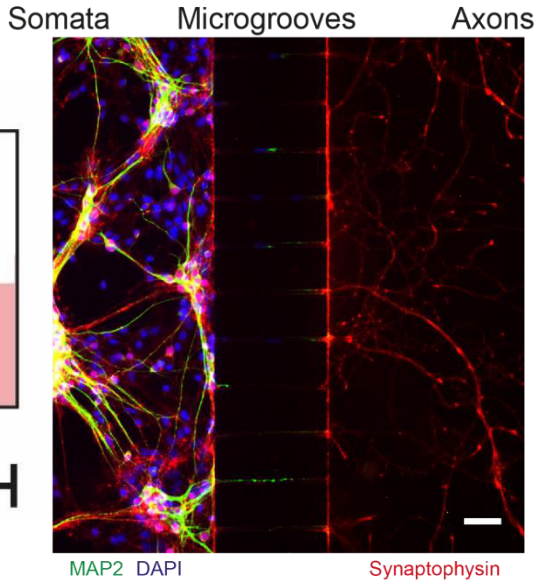

Scale bar = 50 µm

Patent (European Patent Office, file number: 20152016.0);
Palumbo et al., Cells, 2021

Studying axonal degeneration after brain hemorrhage

Alex Palumbo

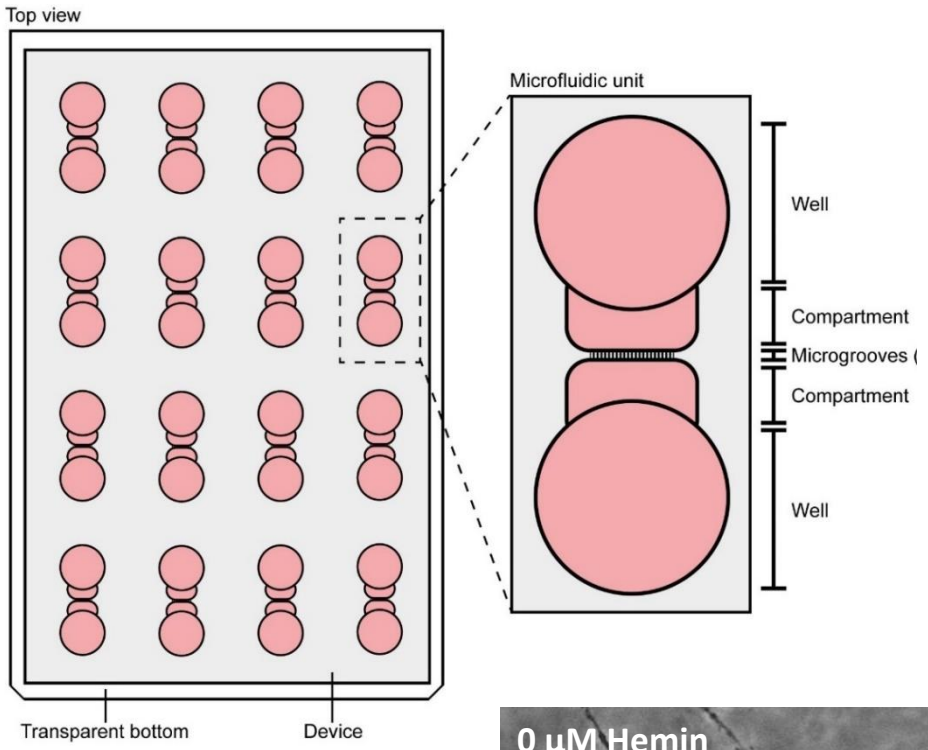

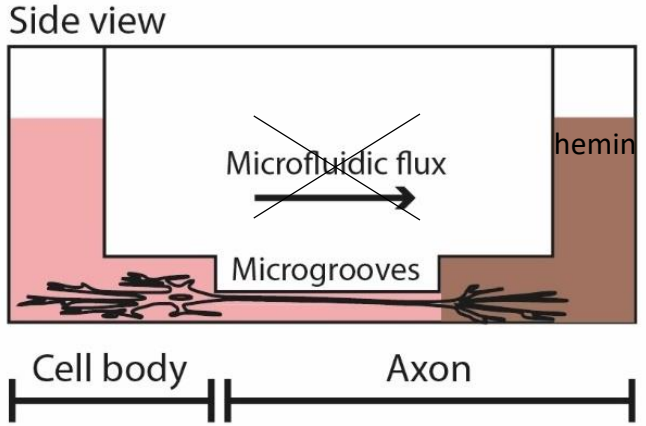

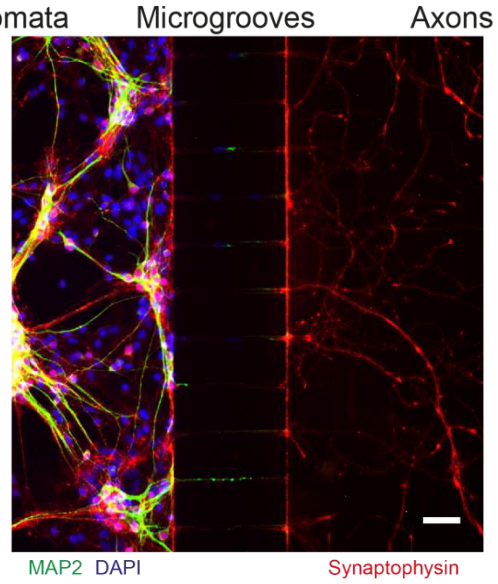

Scale bar = 50 µm

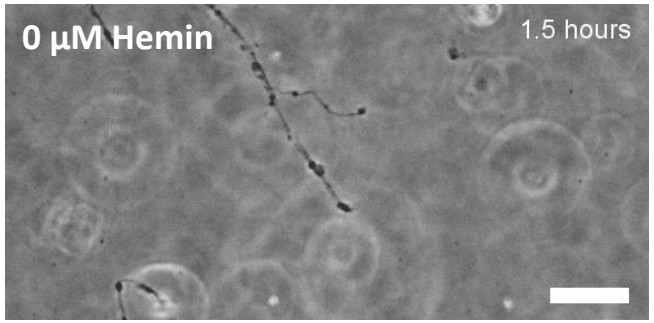

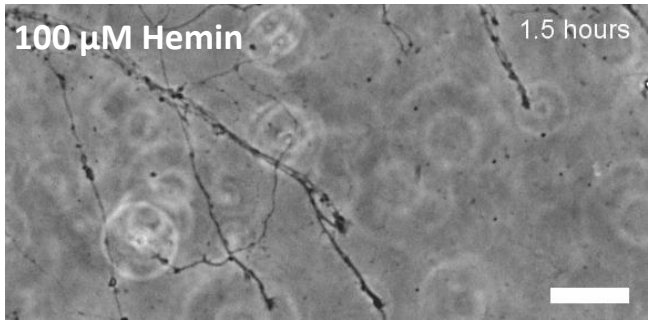

Patent (European Patent Office, file number: 20152016.0);
Palumbo et al., Cells, 2021

Quantitative analysis of axonal degeneration using deep learning: EntireAxon CNN

Philipp Gruening

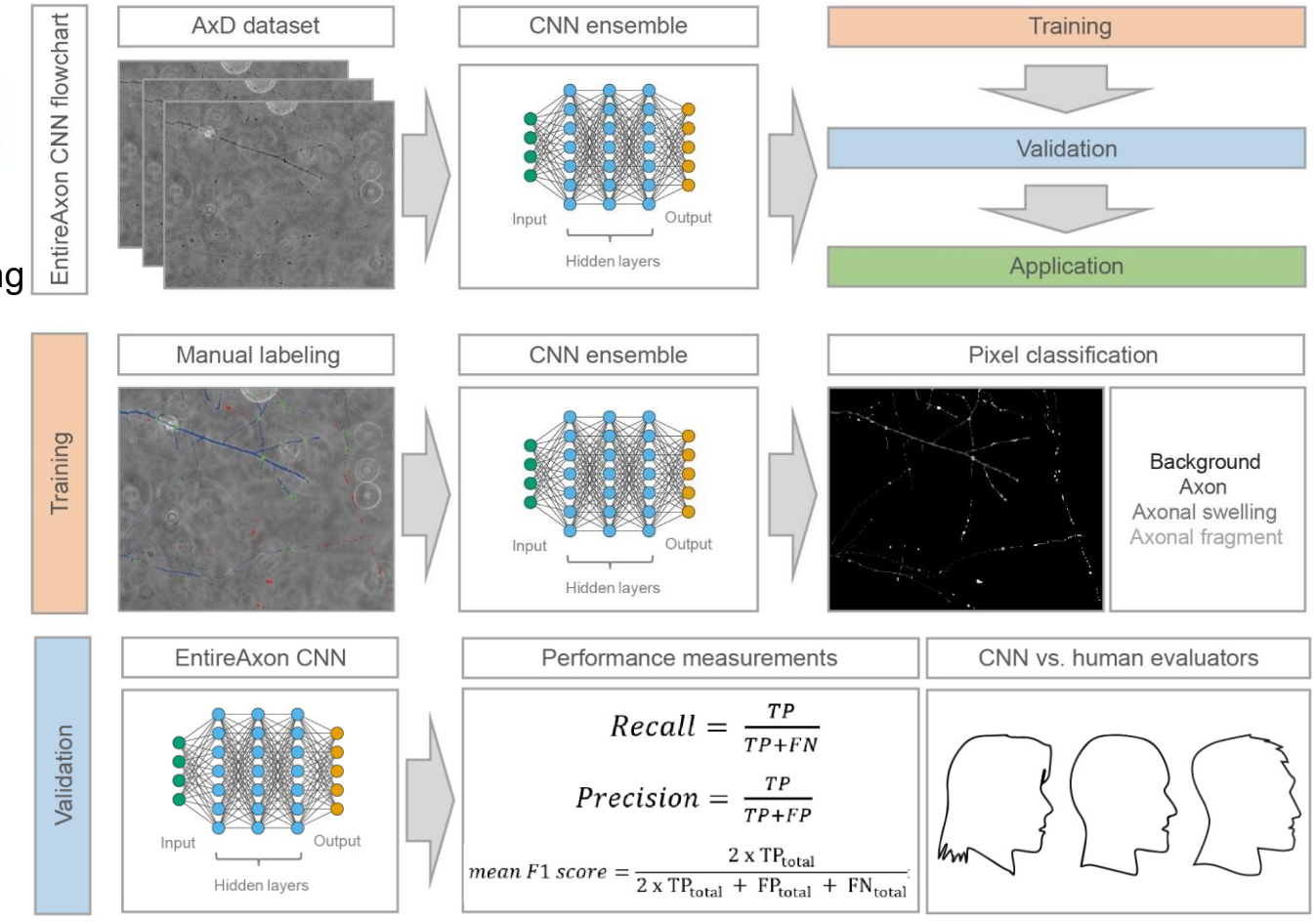

Amir Madany Mamlouk

Patent (European Patent Office, file number: 20152016.0)
Grüning et al., 2020a; Menon et al., 2020; Grüning et al., 2020b; Palumbo et al., Cells, 2021

Hemin induces axonal degeneration in a time- and concentration-dependent manner

Alex Palumbo

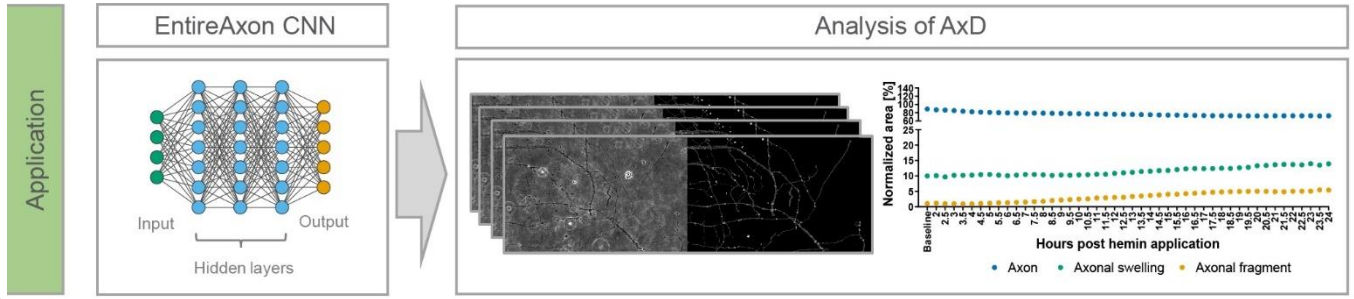

Narayan Kumar Menon

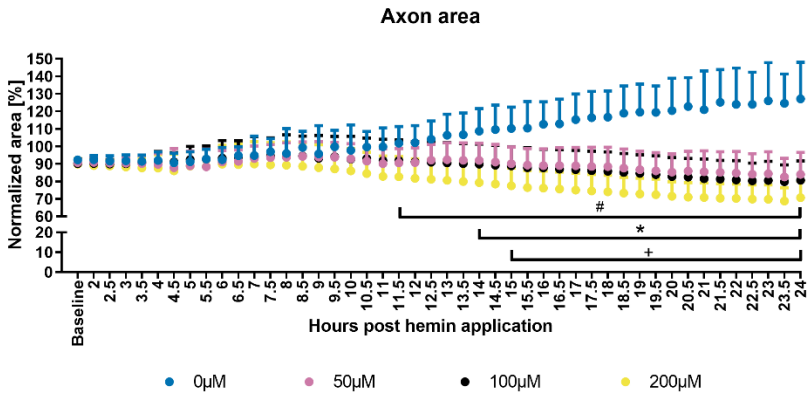

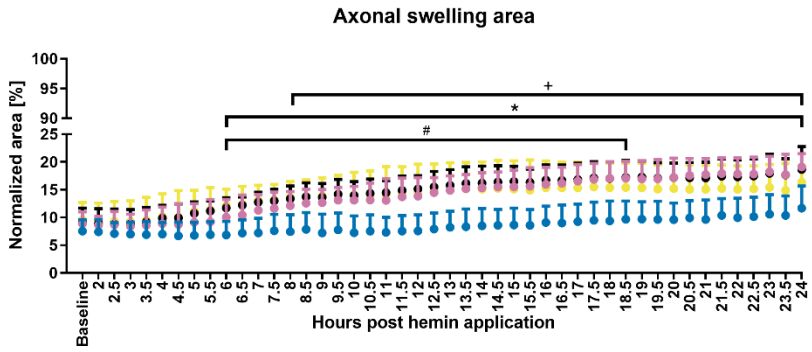

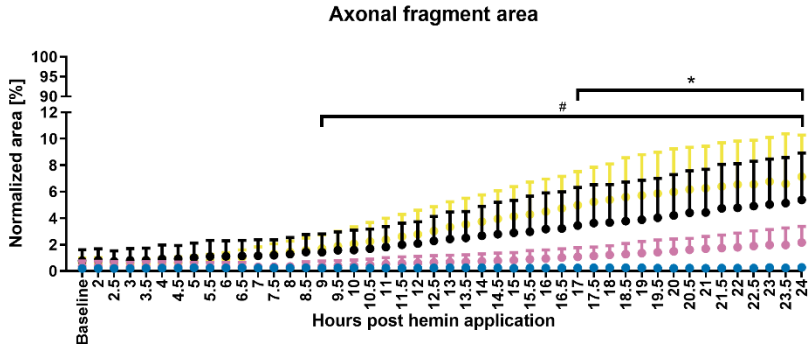

$p < 0.05$, * = 0µM vs 200µM, # = 0µM vs 100µM,
+ = 0µM vs 50µM, n = 6

Menon et al., 2020; Palumbo et al., Cells, 2021

Do degenerating axons show features of ferroptosis?

Expression of ferroptotic markers in hemin-induced AxD

Alex Palumbo

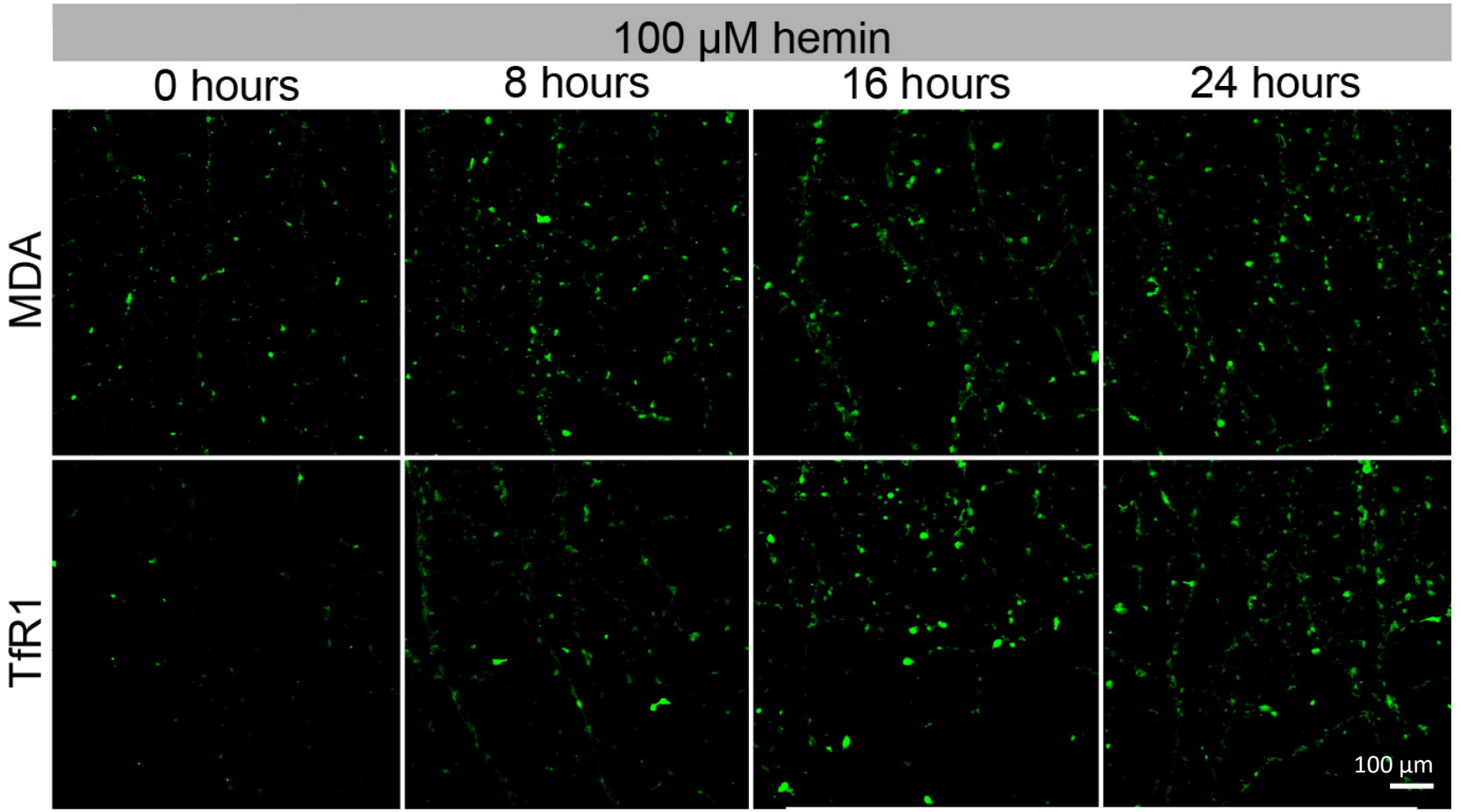

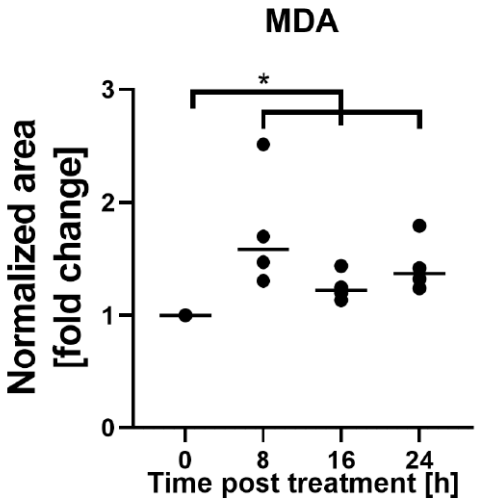

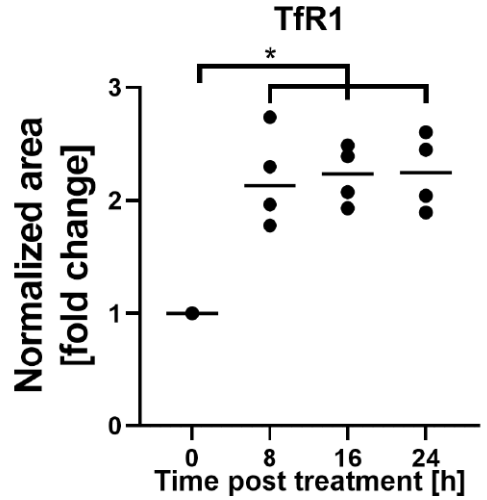

MDA – malondialdehydes, TfR1 – transferrin receptor 1

unpublished data

Do inhibitors of ferroptosis abrogate hemin toxicity to axons?

Ferroptosis inhibitors do not protect against hemin-induced axonal degeneration

Alex Palumbo

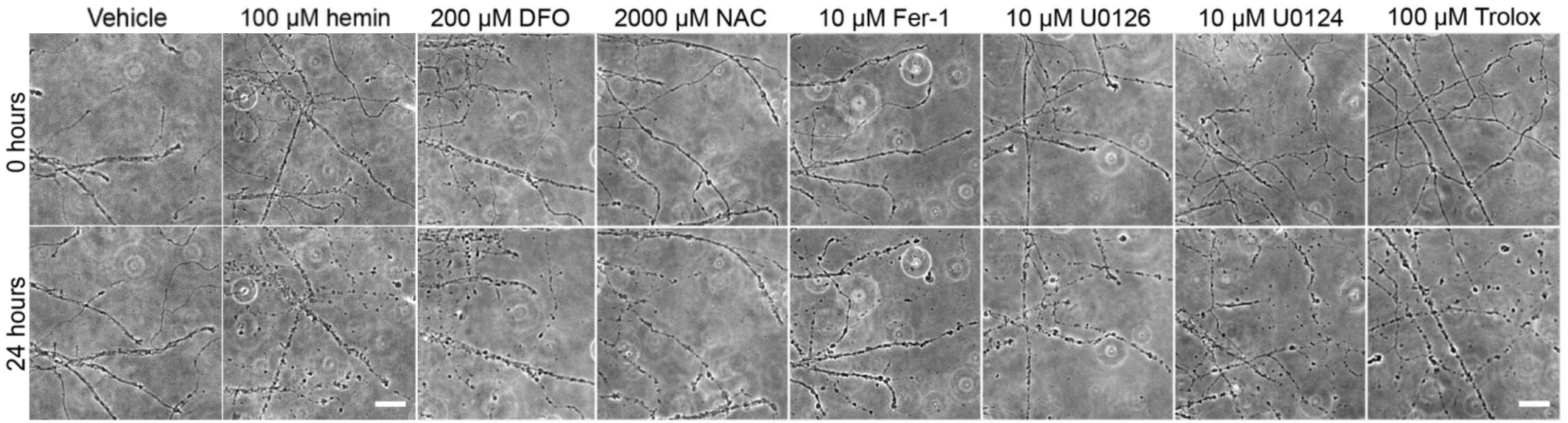

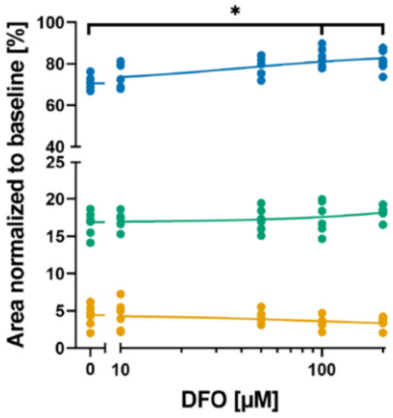

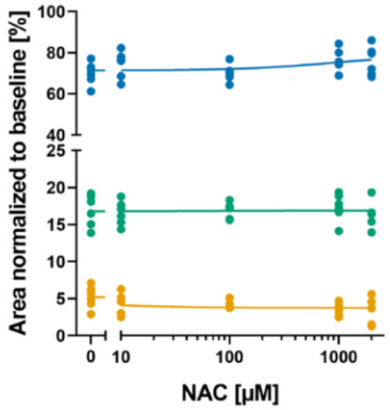

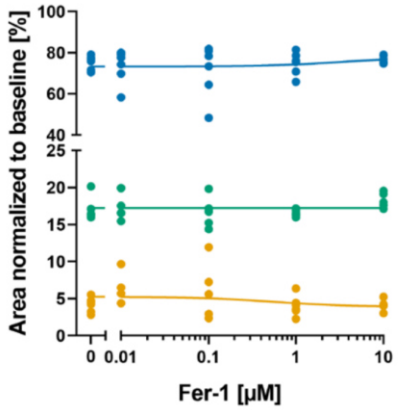

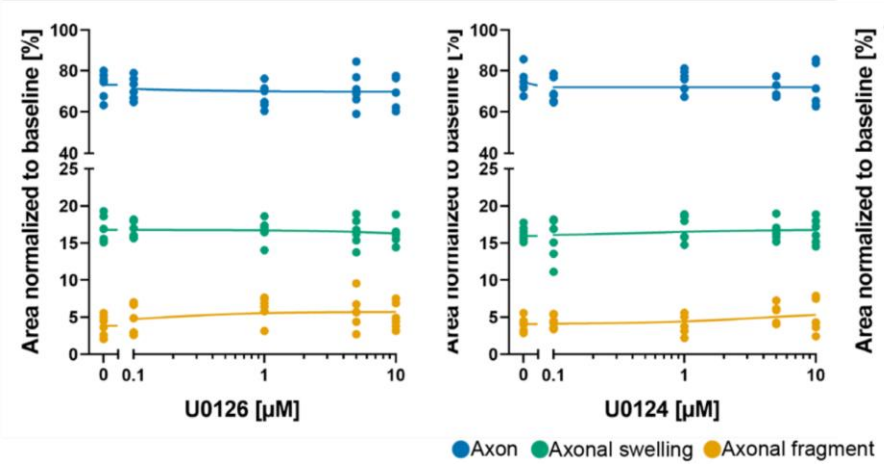

unpublished data

Conclusions

- Clot-derived neuronal toxicity after ICH shares features of ferroptosis and necroptosis
- Studying the rich biology of cell death mechanisms gives rise to novel therapeutic approaches, including combinatorial strategies
- The mechanisms of death of the neuronal cell body may be different from axonal degeneration that may be different from brain endothelial cell death

→ We need to target multiple cell types and compartments for therapeutic approaches to be successful in hemorrhagic stroke

Proposed model for a combinatorial therapy in ICH

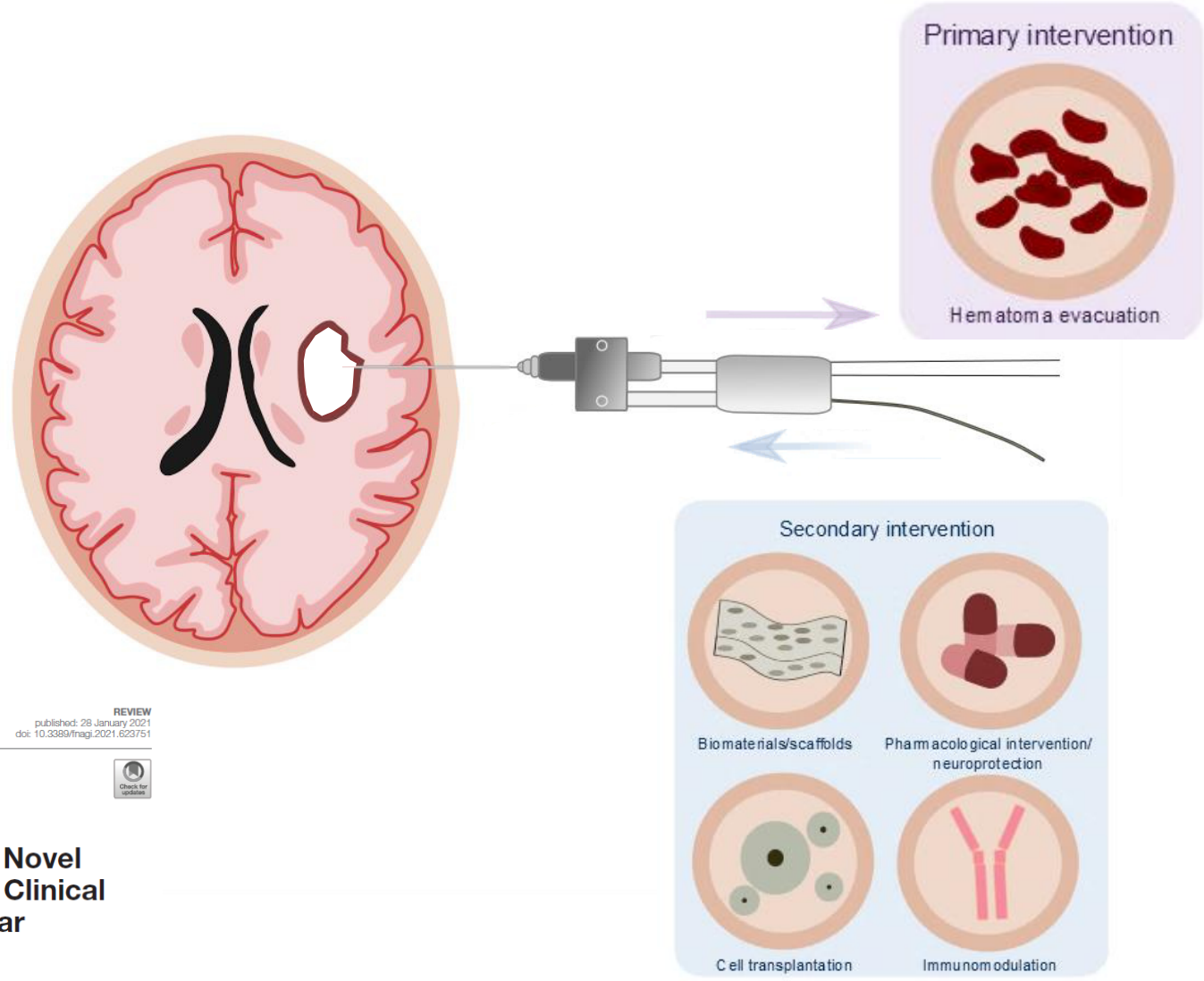

frontiers in Aging Neuroscience

REVIEW
published: 28 January 2021
doi: 10.3389/fnagi.2021.623751

New Mechanistic Insights, Novel Treatment Paradigms, and Clinical Progress in Cerebrovascular Diseases

Boltze, …., Zille, Front Aging Neurosci, 2021

universität wien

@ZilleMarietta

Acknowledgements

Zille Lab
(Current & Former)

Amir Pasokh
Hari Baskar Balasubramanian
Dr. Alex Palumbo
Dr. Maulana Ikhsan
Alessa Pabst
Svenja Landt
Lara Heckmann
Inga Hellige
Sören Pietsch
Narayan Kumar Menon
Katja Grau
Frederike Heiden
Floradel Bürgel
Sirjan Chhatwal
Sarah Grabner
Sarah Hinterhölzer
Johann Nguyen
Dominik Kahr
Julia Fastner

Collaborators

Rajiv R. Ratan, Burke/Cornell, USA
Amit Kumar
Saravanan Karuppagounder
Yingxin Chen

Alma L. Burlingame, U California, USA
Juan A. Oses-Prieto

Sara R. Savage,
Baylor College of Medicine, USA

Amir Madany Mamlouk, U Luebeck, GER
Philipp Gruening

Markus Schwaninger, U Luebeck, GER
Josephine Lampe

JOACHIM HERZ STIFTUNG

DFG Deutsche Forschungsgemeinschaft

Bundesministerium für Bildung und Forschung

Fraunhofer

ÖAW AUSTRIAN ACADEMY OF SCIENCES

City of Vienna